Analysis of Dynamic Measurements

- Evaluation of dynamic measurement uncertainty -

vorgelegt von
Diplom-Mathematiker
Sascha Eichstädt
Frankenberg/Hainichen

Von der Fakultät II - Mathematik und Naturwissenschaften
der Technischen Universität Berlin
zur Erlangung des akademischen Grades
Doktor der Naturwissenschaften
Dr. rer. nat.

genehmigte Dissertation

Promotionsauschuss:

Vorsitzender: Prof. Dr. rer. nat. Dieter Breitschwerdt
Berichter: Prof. Dr. rer. nat. Eckehard Schöll
Berichter: Prof. Dr. rer. nat. Markus Bär
Berichter: Dr. rer. nat. Clemens Elster

Tag der wissenschaftlichen Aussprache: 28. Februar 2012

Berlin 2012
D 83

Abstract

Metrology is concerned with the establishment of measurement units and the transfer of measurement standards to industry. International comparability of measurement results requires internationally agreed guidelines for specific measurement tasks and a standardised treatment of measurement uncertainties. To this end, the *Guide to the Expression of Uncertainty in Measurement* (GUM) provides the framework for the evaluation and interpretation of measurement uncertainty in metrology. However, it does not address dynamic measurements, which are of growing importance for industry and metrology. Typical examples of dynamic measurements are in-cylinder measurements in the automotive industry (pressure), crash tests (e.g., acceleration and force) or assembly line measurements (e.g., torque and force). A reliable calibration of the measurement systems employed, which can be related to national standards, requires a consistent evaluation of measurement uncertainty for dynamic measurements.

The goal of this thesis is to develop a framework for the evaluation of uncertainty in dynamic measurements in metrology that are closely related to the treatment of static measurements. The measurement systems considered are those that can be modelled by a linear and time-invariant (LTI) system since such models cover a wide range of metrological applications. The measured values are the values of the system output signal, whereas the values of the quantity of interest serve as the system input signal. Estimation of the input signal is considered to be carried out by means of digital filtering in the discrete time domain from which inference of the continuous-time signal is sought.

This requires the design of digital filters, an uncertainty evaluation for regularised deconvolution and a framework for the definition and propagation of the uncertainty of a continuous function. The design of digital filters for deconvolution is well-established in the signal processing literature. The same holds true for the propagation of variances through LTI systems. However, propagation of variances through uncertain LTI systems for evaluation of uncertainty in the sense of GUM has only recently been considered. The methods developed so far focus on the evaluation of uncertainties and do not address regularisation errors. Moreover, the relation of the discrete-time estimate to the actual continuous-time measurand has not yet been addressed.

We extend the available results for the evaluation of uncertainties to the propagation of associated probability density functions and propose efficient calculation schemes. Moreover, the ill-posed deconvolution problem requires regularisation. We develop a reliable quantitative evaluation of the uncertainty contribution due to regularisation assuming a particular type of prior knowledge. We present a framework for the evaluation of uncertainty for continuous measurements, which addresses the definition, assignment and propagation of uncertainty. Finally, we develop a technique for the calculation of uncertainty associated with a continuous-time estimate of the measurand from a discrete-time estimate.

The proposed techniques provide a complete framework for the consistent and reliable evaluation of uncertainty in the analysis of a dynamic measurement.

Zusammenfassung

Die Metrologie beschäftigt sich mit der Etablierung von Maßeinheiten und dem Transfer von Standards in die Industrie. Für die internationale Vergleichbarkeit von Messergebnissen werden international akzeptierte Richtlinien für spezifische Messaufgaben benötigt, sowie ein standardisiertes Verfahren zur Bestimmung von Messunsicherheiten. Zu diesem Zweck stellt der *Guide to the Expression of Uncertainty in Measurement* (GUM) einen Rahmen bereit für die Auswertung und Interpretation von Messunsicherheit in der Metrologie. Er behandelt jedoch nicht dynamische Messungen, welche von wachsender Bedeutung für die Industrie und Metrologie sind. Typische Beispiele für dynamische Messungen sind *in-cylinder* Messungen in der Automobilindustrie (Druck), Crash-Tests (z.B. Beschleunigung und Kraft) und Fließband-Messungen (z.B. Drehmoment und Kraft). Rückführbare und zuverlässige Kalibrierung der eingesetzten Messsysteme erfordert eine konsistente Ermittlung der Messunsicherheit für dynamische Messungen.

Das Ziel dieser Arbeit ist es, einen Rahmen für die Ermittlung der Unsicherheit in dynamischen Messungen zu entwickeln, der eng mit der Behandlung von statischen Messungen in der Metrologie steht. Dazu werden Messsysteme betrachtet, die durch ein lineares und zeitinvariantes (LTI) Modell approximiert werden können, da diese Modelle eine breite Palette von Anwendungen in der Metrologie abdecken. Die Messgröße ist dabei das Eingangssignal des Systems. Die Schätzung der Werte der Messgröße erfolgt mittels digitaler Filterung im diskreten Zeitbereich, von welchem Rückschluss über die zeitkontinuierliche Messgröße zu ziehen ist.

Dies erfordert den Entwurf digitaler Filter zur Entfaltung, die Ermittlung der Unsicherheit für die regularisierte Entfaltung und die Definition und Fortpflanzung der Unsicherheit einer stetigen Funktion. Der Entwurf digitaler Filter für die Entfaltung ist in der Signalverarbeitungsliteratur etabliert, ebenso die Fortpflanzung von Varianzen durch lineare dynamische Systeme. Jedoch ist die Fortpflanzung von Varianzen durch unsichere dynamische Systeme im Sinne des GUM ein relativ neues Thema. Die bisher entwickelten Methoden behandeln lediglich die Bestimmung von Standardunsicherheiten und berücksichtigen nicht den Unsicherheitsbeitrag des Regularisierungsfehlers. Außerdem behandeln die bisherigen Untersuchungen nicht die Beziehung der zeitdiskreten Schätzung zu der tatsächlichen zeitkontinuierlichen Messgröße.

Wir erweitern die Ergebnisse für die Bestimmung von Standardunsicherheiten zu einer Bestimmung von multivariaten Wahrscheinlichkeitsdichtefunktionen und entwerfen dafür effiziente Berechnungsmethoden. Zur Regularisierung des schlecht gestellten Problems der Entfaltung entwickeln wir eine Methode, welche die quantitative Bestimmung des zugehörigen Unsicherheitsbeitrags ermöglicht. Wir präsentieren einen Rahmen für die Auswertung kontinuierlicher Messungen, welcher die Definition, Zuordnung und Fortpflanzung von Unsicherheiten behandelt. Des weiteren entwickeln wir eine Methodik für die Fortpflanzung der Unsicherheit einer zeitdiskreten Schätzung der Messgröße in den Raum der stetigen Funktionen.

Contents

List of Figures

List of Abbreviations

GUM	Guide to the Expression of Uncertainty in Measurement
GUM-S1	Supplement 1 to the GUM
GUM-S2	Supplement 2 to the GUM
PDF	Probability Density Function
LTI	Linear Time Invariant (system)
ADC	Analogue-to-Digital Converter
DSP	Digital Signal Processing
FIR	Finite length Impulse Response
IIR	Infinite length Impulse Response

List of Symbols

$\mathbb{R}^n$	n-dimensional space of real numbers
$\mathbb{Z}$	space of integers
$\mathbb{C}$	space of complex numbers
j	imaginary unit $\sqrt{-1}$
$C(I, \mathbb{R})$	space of continuous functions from interval I to $\mathbb{R}$
$x(t)$	time-dependent function
T_s	sampling interval length
$x[n]$	evaluation of $x(t)$ at nth sample point: $x(nT_s)$
$\mathbb{P}$	probability measure
p_y	probability density function w.r.t. y
$\mathbb{E}$	mathematical expectation
X	(univariate) random variable
$\hat{x}$	estimate of X
$u(\hat{x})$	uncertainty associate with $\hat{x}$
$\mathbf{X}$	random vector
$U_{\hat{\mathbf{x}}}$	uncertainty (covariance matrix) associated with estimate of $\mathbf{X}$
$\mathbf{x}^\top$	transposed vector
X_t	continuous-time stochastic process
$X(t, \omega)$	stochastic process evaluated at (t, ω)

Introduction

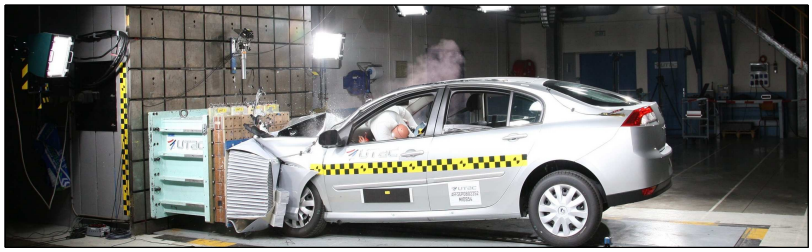

Figure 1: Example of a dynamic measurement involving the measurement of dynamic acceleration and shock force (photo Christophe Bertolin)

Metrology – the science of measurement – is concerned with the establishment of measurement units, the realisation of measurement standards and the transfer of these standards to industry by means of calibration. The acceptance of testing and calibration measurement results between different countries is the key to an efficient global economy. In this regard, the World Trade Organization (WTO) has also recognised that the lack of international comparability is a significant *technical barrier to trade* [1]. Moreover, the *Bureau international des poids et mesures* (BIPM) states that the "economic success of nations depends upon the ability to manufacture and trade precisely made and tested products and components" [2]. This requires the comparability of measurements starting from the inter-laboratory level up to an international level, which is denoted as "traceability". The BIPM defines traceability to mean "that the result of a measurement, no matter where it is made, can be related to a national or international measurement standard, and that this relationship is documented" [2]. To this end, a number of standard documents have been developed, which set out internationally agreed guidelines for specific measurement tasks. One particular document, namely the *Guide to the Expression of Uncertainty in Measurement* (GUM) [3], provides a framework for an internationally harmonised evaluation and interpretation of measure-

ment uncertainty. The GUM has been developed by an international group of standard bodies in line with an initiative of the BIPM and a number of national metrology institutes (NMI). Ongoing amendments are made to this guide by means of revisions and supplementary documents [4–6].

The GUM and its current supplements do not directly address the measurement of quantities considered here, whose values show a significant time dependence. That is why there has been a significant lack of traceability for dynamic measurements up to now. However, dynamic measurements are becoming increasingly important in industry and metrology since many applications of measurement devices are used in a highly dynamic environment [7]. This lack of traceability and calibration services has been recognised, for instance, by ISO 6487 "Road Vehicles – Measurement techniques in impact tests – Instrumentation", the EURAMET "Technical Committee for Mass and Related Quantities" and the "Joint Committee for Guides in Metrology". The impact of this lack of traceability is that many measurement systems are calibrated under static conditions, but are employed for dynamic measurements. Therefore, a number of international projects have been initiated, which aim at the establishment of traceability for dynamic measurements. A recent example is the European Metrology Research Programme (EMRP) project "Traceable Dynamic Measurement of Mechanical Quantities" [8]. It aims at the establishment of traceability for dynamic measurements of force, torque and pressure. Typical examples for measurements of these quantities are in-cylinder car engine measurements, assembly line measurements or crash tests. One of the largest work packages in this project is the development of methods for the evaluation of dynamic uncertainty. Thus, mathematics plays a key role in the successful establishment of traceability.

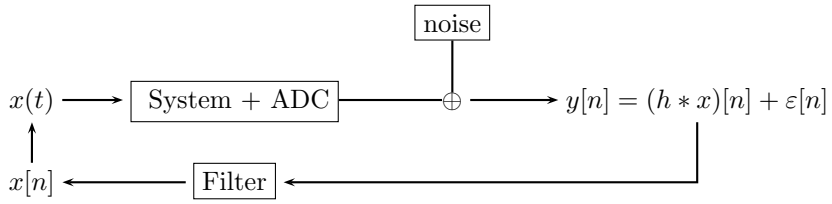

Figure 2: Workflow in the analysis of a dynamic measurement. The continuous-time value of the measurand is the input signal to the dynamic measurement system. It subsequently undergoes an analogue-to-digital conversion (ADC) and is disturbed by noise. Estimation of a discrete-time variant of the input signal is carried out by means of digital filtering. Inference of the continuous-time measurand is then made from the discrete-time estimate.

The goal of this thesis is the development of methods for the extension of the current guidelines for the evaluation of measurement uncertainty of dynamic measurements according to Fig. 2. The thesis focuses on measurement systems which can be assumed to be linear and time-invariant (LTI), since such system models cover a wide range of applications in metrology [9–12]. The typical analysis of a dynamic measurement is depicted in Fig. 2. The measurand is the continuous function $x(t)$. The system output signal subsequently undergoes an analogue-to-digital conversion (ADC) resulting in noise disturbed discrete-time observations $y[n] = y(nT_s)$, where T_s is the chosen sampling interval length. The goal is to estimate the value of the measurand, which served as input signal to the system. To this end, a linear estimation in the discrete-time domain by means of digital filtering is considered; cf. [13]. This requires the design of digital deconvolution filters and an appropriate evaluation scheme for the associated uncertainties. The design of digital filters for deconvolution is well-established in the digital signal processing (DSP) literature [13–15]. For the evaluation of the resulting uncertainties in line with the guidelines, closed formulas have recently been developed [16, 17]. However, these methods do not consider the systematic errors introduced by the deconvolution as a result of the ill-posedness of the estimation problem. Moreover, the relation of the discrete-time estimate $\hat{x}[n]$ to the actual continuous-time measurand $x(t)$ is not addressed.

To this end, we extend the results for the evaluation of uncertainties to the propagation of associated probability density functions and propose efficient calculation schemes. Moreover, we develop a reliable evaluation of the uncertainty contribution of regularisation for a specific type of prior knowledge. We present a framework for the evaluation of uncertainty for continuous measurements, which addresses the definition, assignment and propagation of uncertainty. Finally, we develop a technique in which we use the discrete-time estimate for the calculation of uncertainty associated with a continuous-time estimate of the measurand. This technique allows for an application of DSP techniques and multivariate probability calculus for the evaluation of measurement uncertainty for the continuous-time measurand.

The thesis is structured as follows. Chapter 1 provides a brief introduction and introduces the notation used. In Chapter 2, a framework is developed for the definition, assignment and propagation of uncertainty in function spaces. Finally, in Chapter 3 an uncertainty evaluation scheme is developed for the estimation of the discrete-time variant of the measurand. In Chapter 4, the proposed methodologies are illustrated by means of applications.

Chapter 1

Preliminaries

Metrology as the science of measurement generally combines various aspects of several different fields of science. In addition, the evaluation of measurement uncertainty comprises certain aspects of statistics. The analysis of dynamic measurements also uses methodologies from signal processing. The goal of this chapter is to summarise the preliminaries from these fields that are required for the subsequent investigations. In this chapter we also introduce the notations used in this thesis. Where possible, we use notations that are typical for the signal processing literature.

1.1 Evaluation of measurement uncertainty

In general, measured values should be accompanied by a quantitative statement on their quality. Such a statement has to allow for a comparison of the measurements themselves or to reference standards. The statement on the quality of measurement in metrology is the *measurement uncertainty*, which expresses the fact that the *true value* of a quantity remains unknown even after a measurement. For the assignment and evaluation of uncertainty, we consider a treatment that is in line with the framework proposed by the GUM and its supplements, GUM-S1 and GUM-S2 [3–5].

Limited knowledge about the value of a quantity is modelled by a random variable, which is characterised by its associated probability density function (PDF).

Definition 1.1 (measurement uncertainty)**.** *Let* $p_{\mathbf{x}} : \mathbb{R}^N \to [0, \infty)$ *denote the probability density function which models the state of knowledge about the value of the quantity*

$$\mathbf{X} = (X_1, \ldots, X_N).$$

The estimate $\hat{\mathbf{x}}$ *of* $\mathbf{X}$ *and its associated uncertainty are defined as*

$$\hat{\mathbf{x}} = \int p_{\mathbf{x}}(\boldsymbol{\xi}) \boldsymbol{\xi} d\boldsymbol{\xi} \tag{1.1}$$

$$U_{\hat{\mathbf{x}}} = \int p_{\mathbf{x}}(\boldsymbol{\xi})(\boldsymbol{\xi} - \hat{\mathbf{x}})(\boldsymbol{\xi} - \hat{\mathbf{x}})^T d\boldsymbol{\xi}, \tag{1.2}$$

where $U_{\hat{\mathbf{x}}}$ *denotes the matrix of mutual uncertainties* $u(\hat{x}_k, \hat{x}_l)$ *for* $k, l = 1, \ldots, N$ *and with* $\hat{x}_k$ *the estimate of* $X[k]$*.*

The evaluation of measurement uncertainty thus requires assigning a probability density function to the measurand. Generally, this can be achieved by means of statistical inference based on measurements/observations and/or prior knowledge about influencing quantities. For instance, in a Bayesian inference one employs Bayes' theorem to update one's state of knowledge, expressed by a PDF, given a new set of data [18].

As a starting point for the measurement analysis, the guidelines in metrology consider the *measurement* model

$$\mathbf{X} = \begin{pmatrix} X_1 \\ \vdots \\ X_N \end{pmatrix} = f(Y_1, \ldots, Y_M) \quad f \in C^1(\mathbb{R}^M, \mathbb{R}^N), \tag{1.3}$$

which relates the measurand $\mathbf{X}$ to a finite number of quantities Y_i which influence the measurement result.

Inference on $\mathbf{X}$ then requires the assignment of a PDF associated with $\mathbf{Y}$ and its propagation through the model function. Typically, knowledge about $\mathbf{Y}$ is available by means of observations, documented standards or prior measurement results. For typical situations in metrological applications, GUM-S1 and GUM-S2 [4, 5] specify the PDF assigned to $\mathbf{Y}$. However, in general this assignment is itself a task of statistical inference. The PDF $p_{\mathbf{x}}$, associated with the value of the measurand, is obtained from the PDF $p_{\mathbf{y}}$ by means of the *change-of-variables* formula for the measurement model [4, 19–21].

Definition 1.2 (PDF calculus)**.** *Assume that a state of knowledge PDF* $p_{\mathbf{y}}(\mathbf{y})$ *has been assigned to the input quantities* $Y_1, \ldots, Y_N$ *and that the measurand* $\mathbf{X}$ *is related to* $\mathbf{Y}$ *by the model function*

$$\mathbf{X} = f(\mathbf{Y}).$$

The PDF $p_{\mathbf{x}}$ *which models the state of knowledge about* $\mathbf{X}$ *is then obtained by application of the change-of-variables formula:*

$$p_{\mathbf{x}}(\boldsymbol{\xi}) = \int p_{\mathbf{y}}(\boldsymbol{\eta})\delta(\boldsymbol{\xi} - f(\boldsymbol{\eta}))d\boldsymbol{\eta}, \tag{1.4}$$

where $\delta(\cdot)$ *is the Dirac delta function.*

Remark 1.1. *The integral (1.4) exists for all* $\boldsymbol{\xi}$ *for which* $|Df(\boldsymbol{\eta})|$ *is non-singular at the roots of* $\boldsymbol{\xi} = f(\boldsymbol{\eta})$ *[20, 21].*

This inference on $\mathbf{X}$ from the input quantities $\mathbf{Y}$ does not account for prior knowledge and requires a functional relationship between the quantity of interest and the observed quantities. The assigned PDFs are interpreted to encode the degree of belief or state of knowledge about the value of the quantity [4], which is related to the point of view in Bayesian statistics. Moreover, it has been shown that in particular situations the PDF associated with the measurand, as obtained by the rules of GUM-S1, coincides with that of a Bayesian inference with standard non-informative priors [19, 22–24].

When the model function (1.3) is linear (or linearised around the estimate $\hat{\mathbf{y}}$) and only an estimate $\hat{\mathbf{x}}$ and its associated uncertainty are to be determined, then a calculation of the integral (1.4) is not required. Instead, a propagation of the uncertainty through (a linearisation of) the model (1.3) can be carried out [3].

Definition 1.3 (Uncertainty calculus)**.** *Assume that the measurand* $\mathbf{X}$ *is related to the input quantities* $\mathbf{Y}$ *by the model function*

$$\mathbf{X} = f(\mathbf{Y}).$$

Assume also that the (mutual) uncertainties $(U_{\hat{\mathbf{y}}})_{k,l} = u(\hat{y}_k, \hat{y}_l)$ *have been associated with an estimate of the input quantities* Y_k *and that an estimate of the measurand* $\mathbf{X}$ *and its associated uncertainty by means of uncertainty calculus are then obtained as*

$$\hat{\mathbf{x}} = f(\hat{\mathbf{y}}) \tag{1.5}$$

$$U_{\hat{\mathbf{x}}} = F U_{\hat{\mathbf{y}}} F^T, \tag{1.6}$$

where the matrix $F \in \mathbb{R}^{N\times M}$ *denotes the linearisation of the mapping* $\mathbf{y} \mapsto f(\mathbf{y})$ *at* $\hat{\mathbf{y}}$.

Evaluation of uncertainty by means of uncertainty calculus is exact for linear models. For significantly non-linear models, the method of PDF calculus is preferred to avoid linearisation errors [4].

Since the integrals (1.1) and (1.2) are hardly tractable analytically, numerical methods, such as Monte Carlo integration, have to be used. Therefore, samples are drawn from the PDF $p_{\mathbf{y}}$ and propagated through the model function (see Fig. 1.1).

$$\left\{\mathbf{y}^{(k)} \sim p_{\mathbf{Y}}(\mathbf{y})\right\}_{k=1}^{N_{MC}} \longrightarrow \boxed{\mathbf{x}^{(\mathsf{k})} = \mathsf{f}(\mathbf{y}^{(\mathsf{k})})} \longrightarrow \left\{\mathbf{x}^{(k)} \sim p_{\mathbf{X}}(\mathbf{x})\right\}_{k=1}^{N_{MC}}$$

Figure 1.1: PDF calculus by means of a Monte Carlo integration method. The resulting model function values $\{\mathbf{x}^{(k)}\}$ are independent sample draws from the PDF $p_{\mathbf{x}}$ sought.

A sufficiently large number of samples then allows us to evaluate equations (1.1) and (1.2) for the estimate and uncertainty, respectively [4]. It is worth noting that contrary to the method of uncertainty calculus, the Monte Carlo integration to carry out PDF calculus is *never* exact owing to its randomness. Hence, the choice of the number of Monte Carlo trials is crucial for the reliability of the obtained uncertainty; cf. [25].

Remark 1.2. *In this thesis we focus on the determination of the measurement model and the* propagation *of uncertainties. That is, we usually assume that a PDF (or an estimate and its associated uncertainty) has been assigned to the input quantities.*

1.2 Dynamic measurements

The guidelines GUM/GUM-S1 consider measurements of quantities which are constant in time. While this is appropriate for a wide range of applications in metrology, there is a growing interest in the measurement of time-varying quantities[1] [7].

[1]Note that the dynamic quantities referred to are only those with time-varying values. However, the results are equivalent for those with spatial-varying values.

Definition 1.4 (Dynamic Measurement)**.** *A measurement is considered to be a* dynamic measurement *when the value of the quantity of interest varies over time.*

The measurement of dynamic quantities is a usual task in many applications, such as thermometer measurements [10], measurements of dynamic acceleration [26] or dynamic force [12, 27] and the calibration of high-speed electronic devices [28–30]. Currently, however, traceability for these quantities only exists for static measurements. Establishing traceability for dynamic measurements requires a calibration of the measurement device, which accounts for its dynamic behaviour [7]. Therefore, calibration measurements have to be performed under suitable dynamic conditions. Moreover, the methods employed for the evaluation of uncertainty have to be consistent with the methodologies for static measurements. That is, in the static limit, when the impact of the dynamics is no longer significant, the results should be consistent with those obtained from a static measurement analysis, e.g., [7, 16].

1.2.1 Dynamic measurement systems

The measurement system in a dynamic measurement in metrology can often be assumed to be linear and time-invariant (LTI), [9–12]. Consequently, we focus on the development of methods for LTI system models. The most important results in this area which are used in this thesis are summarised below. For more detailed information, refer to [13, 14].

Continuous-time LTI systems

In general, a linear dynamic system can be viewed as some linear operator on the function space of potential input signals. Often, the relation between input and output can be modelled by an ordinary differential equation (ODE). The relation between input and output signal is then given by the integral operator equation [14]

$$y(t) = H\{x(t)\} = \int_{-\infty}^{\infty} h(t,\tau)x(\tau)d\tau.$$

For time-invariant systems, i.e., ODEs with constant coefficients, this can be simplified to the continuous-time convolution

$$y(t) = H\{x(t)\} = \int_{-\infty}^{\infty} h(t-\tau)x(\tau)d\tau = (h * x)(t),$$

where the operator kernel function $h(t)$ is called the impulse response of the LTI system. That is, $h(t)$ is the response of the system to a Dirac delta function. In practice, the systems that are considered are those for which the current value of the output only depends on present and past values of the input. Such systems are called *causal* and the corresponding integral equation becomes

$$y(t) = H\{x(t)\} = \int_{-\infty}^{t} h(t-\tau)x(\tau)d\tau.$$

The transfer function as a mathematical model for the input-output relation of a (continuous-time) LTI system is usually given as a Laplace transform of the corresponding differential equation

$$H(s) = \frac{\sum_{k=0}^{N} \tilde{b}_k s^k}{\sum_{k=0}^{M} \tilde{a}_k s^k}. \tag{1.7}$$

A continuous-time LTI, system is called stable if all poles of its rational Laplace domain transfer function are located in the left half plane of $\mathbb{C}$. A LTI system is called minimum-phase if it is stable and if its inverse is also stable [13].

Discrete-time LTI systems

For a discrete-time LTI system, the relation between (discrete-time) input and output signal is given by

$$y[n] = \sum_{k=-\infty}^{\infty} h[n-k]x[k] = (h * x)[n], \tag{1.8}$$

where $(h[k])_{k\in\mathbb{Z}}$ is the discrete-time impulse response of the system. The transfer function $H(z)$ is given by the z-transform of the impulse response

$$H(z) = \sum_{k=-\infty}^{\infty} h[k] z^{-k}.$$

and is often expressed in a rational form similar to its Laplace domain counterpart

$$H(z) = \frac{\sum_{k=0}^{N1} b_k z^{-k}}{\sum_{k=0}^{N2} a_k z^{-k}}.$$

A discrete-time LTI system is called stable if all poles of its rational z-domain transfer function are located inside the unit circle in $\mathbb{C}$.

LTI systems can also be represented by a so-called state-space model

$$\mathbf{z}[n+1] = A\mathbf{z}[n] + Bx[n] \tag{1.9}$$
$$y[n] = C\mathbf{z}[n] + Dx[n]. \tag{1.10}$$

In this model, the state variable $\mathbf{z}[n]$ encodes the state of the system at time instant nT_s. The state equation (1.9) thus models the internal dynamics of the LTI system driven by the external input signal $x[n]$. The observations (1.10) are then determined by the state of the system and the input signal.

Frequency response

From the transfer functions $H(s)$ and $H(z)$, respectively, the frequency response of the LTI system is obtained as

$$H(j\Omega) = H(s)|_{s=j\Omega}$$

and respectively for a discrete-time system

$$H(e^{j\omega}) = H(z)|_{z=e^{j\omega}},$$

where $\omega = \Omega T_s$ denotes normalised radial frequency with T_s as the chosen sampling interval in the time domain [13].

Digital filters

Discrete-time LTI systems are usually applied by means of digital filtering. For causal finite-length impulse response (FIR) systems, i.e., $h[k] = 0 \forall k > N$ for a certain $N > 0$, the discrete convolution (1.8) reduces to the finite summation

$$y[n] = \sum_{k=0}^{N} b_k x[n-k], \tag{1.11}$$

with the FIR filter parameters $b_k, k = 0, \ldots, N$ given as the values of the impulse response.

For infinite-length impulse response (IIR) systems, the convolution equation (1.8) is often considered in a recursive form

$$y[n] = \sum_{k=0}^{N1} b_k x[n-k] - \sum_{k=1}^{N2} a_k y[n-k] \quad , \tag{1.12}$$

where the filter parameters $(a_1, \ldots, a_{N2}, b_0, \ldots, b_{N1})$ correspond to the coefficients of the LTI system's z-transform in its rational form, normalised such that $a_0 = 1$.

1.2.2 Dynamic calibration

Calibration of a dynamic system is carried out by dynamic excitations of the system and a non-parametric or parametric regression. Then the system is calibrated by means of a parametric regression to determine an estimate of the system parameters and evaluate their associated uncertainty. This can be realised by means of a Bayesian inference or by considering a least squares approach as in [12, 26]. Another possibility is the measurement of the frequency response function at specific frequency points, typically by sinusoidal excitations, or the impulse response at discrete-time samples as the inverse Fourier transform of the frequency response, e.g., [28, 31]. The estimate of the system is then reported in terms of the impulse response

or frequency response values and their associated (mutual) uncertainties are evaluated by means of uncertainty calculus [31] or PDF calculus [28].

1.2.3 Deconvolution

A model for the observation of the output signal of a discrete-time LTI system is given by the convolution equation [14]

$$y[n] = (h * x)[n] + \varepsilon[n],$$

where $\varepsilon[n]$ denotes a (discrete-time) noise process. Estimation of the value of the measurand $x[n]$ for some $n \in \mathbb{N}$ then requires a deconvolution. Various approaches for the solution of the deconvolution problem exist, an overview of which can be found in [32]. In general, the deconvolution problem is ill-posed and requires some kind of regularisation. Classical approaches are the Wiener deconvolution filter for wide-sense stationary stochastic processes and the Tikhonov regularisation. The frequency response of the Wiener deconvolution filter is given by [33]

$$G(j\Omega) = \frac{H^*(j\Omega)X(j\Omega)}{|H(j\Omega)|^2 X(j\Omega) + N(j\Omega)} \tag{1.13}$$

and a Tikhonov regularisation [34] in the frequency domain results in the following frequency response function [29]

$$G(j\Omega) = \frac{H^*(j\Omega)}{|H(j\Omega)|^2 + \lambda^2 |L(j\Omega)|^2}, \tag{1.14}$$

where H^* denotes complex conjugation, $X(j\Omega)$ and $N(j\Omega)$ denote the power spectrum of the signal process and noise process, respectively, and $L(j\Omega)$ denotes the Fourier transform of a chosen penalty operator.

These approaches for regularised deconvolution can be interpreted as a cascade of the inverse of the measurement system model and a low pass filter. That is, the Wiener deconvolution filter frequency response (1.13) can be written as

$$G(j\Omega) = H^{-1}(j\Omega) \frac{|H(j\Omega)|^2}{|H(j\Omega)|^2 + N(j\Omega)/X(j\Omega)}$$

and for the Tikhonov regularisation (1.14), the decomposition is given by

$$G(j\Omega) = H^{-1}(j\Omega)\frac{|H(j\Omega)|^2}{|H(j\Omega)|^2 + \lambda^2|L(j\Omega)|^2}.$$

Hence, the low pass filter for the Wiener filter is determined by the signal-to-noise ratio, whereas that of the Tikhonov regularisation is determined by the employed penalty operator. As a generalisation, we consider an approximation of the inverse measurement system by a digital filter followed by some low pass filter (see Section 3.2).

A recent comparison study on the application of Tikhonov regularisation in the context of metrology is given in [35]. The authors conclude that there is a significant lack of quantitative results on the quality of generally applied regularisation schemes under realistic conditions. However, that is required in order to evaluate the uncertainty contribution of the regularisation error (see Section 3.5).

1.2.4 Application of GUM for dynamic measurements

The GUM does not address the analysis of dynamic measurements directly. Nevertheless, the underlying methodologies can be extended to the application for discrete-time deconvolution. The measurand is then either the sequence $\mathbf{X} = (X[0], X[1] \ldots, X[N])$ or one particular time sample point $X[k]$. The input quantities are the sequences $\mathbf{Y} = (Y[0], Y[1], \ldots, Y[N])$ and $\mathbf{h} = (h[0], h[1], \ldots, h[M])$ of the system's output signal and the impulse response, respectively. However, in order to apply the guidelines to the estimation of the measurand, the difficulties described below need to be addressed.

Regularisation

The model $\mathbf{X} = f(\mathbf{h}, \mathbf{Y})$ for the evaluation of the measurand $\mathbf{X}$ denotes a deconvolution. Due to the ill-posedness of the deconvolution problem, the estimate of the measurand depends on the chosen regularisation scheme. Thus, the estimate of the measurand are not unique. Moreover, accounting for regularisation errors in the uncertainty budget requires some prior knowledge about the measurand.

Finiteness

The guidelines consider model functions with a finite number of parameters. However, for IIR deconvolution filters the impulse response $\mathbf{h}$ is of infinite length. To this end, the model function has to be formulated in terms of a state-space equation (1.9) and (1.10), or considered in the form (1.12). However, strictly speaking, the resulting model function then considers only a particular time sample point $x[k]$ as measurand (see Section 3.3).

Discretisation

In general, the measurand $x(t)$ is continuous in time, although the observations $y[n]$ are usually obtained as a discrete-time sequence. Reconstruction of a continuous signal $x(t)$ from its discrete counterpart $x[n]$ is considered in standard signal processing literature [13, 14]. However, the uncertainty associated with the discrete-time estimate $\hat{x}[n]$ has to be propagated to a corresponding continuous-time estimate $\hat{x}(t)$. Therefore, a framework for the assignment and evaluation of uncertainty for continuous functions is required.

Chapter 2

Uncertainty evaluation for continuous functions

The considered analysis of a dynamic measurement, as depicted in Fig. 2, is based on an estimation procedure in the discrete-time domain. However, the actual measurand is a continuous function. Hence, a complete measurement analysis needs to relate the discrete-time estimation result $\hat{x}[n]$ in Fig. 2 to the continuous function $x(t)$. Therefore, we define the uncertainty of a (deterministic) function and derive a framework for its evaluation as a consistent extension of the methodologies presented in Section 1.1.

2.1 Continuous function as measurand

Many metrological applications require an estimation of continuous functions. However, the current guidelines in metrology only consider estimation of a finite number of parameters. Therefore, an approximation of the continuous function is usually carried out in terms of discretisation or parametrisation. The measurement result is then reported and transferred in terms of the parameter estimates and their associated uncertainties (uncertainty calculus) or a probability density function modelling the state of knowledge about the values of the parameters (PDF calculus), respectively. Strictly speaking, the reported measurement result is then not a characterisation of the actual measurand, but that of the chosen approximated measurand.

For instance, in the analysis of a dynamic measurement, estimation of a discretised variant $x[n] = x(nT_s)$ of the continuous-time measurand $x(t)$ is considered for a chosen sampling interval length T_s. The measurement result is then reported in terms of the vector-valued estimate $\hat{\mathbf{x}} = (\hat{x}[0], \ldots, \hat{x}[N])$ of the discrete-time signal on a finite interval and its associated covariance matrix (uncertainty calculus) or an associated multivariate probability distribution (PDF caclulus), respectively. The reported measurement result then characterises the particular discretisation of the measurand $x(t)$.

Example 2.1. *Consider the value of a physical quantity (e.g., temperature) measured continuously over time for monitoring purposes. The measurand is then a continuous function $x(t)$. Assume that the measurement model is given by*

$$x(t) = y(t) + c \tag{2.1}$$

with c representing a systematic correction and $y(t)$ the uncorrected continuous-time observation. Reporting the measurement result in terms of a certain discretisation may not be appropriate to characterise the measurand. Evaluation of uncertainty then requires assigning an uncertainty to an estimate of the continuous function $y(t)$ and its propagation through the measurement model.

Assignment of uncertainty to a continuous function is often carried out in terms of a parametrisation. Therefore, let $\boldsymbol{\theta} = (\theta_1, \ldots, \theta_M)$ denote a finite-dimensional parameter vector such that the measurand $x(t)$ can be expressed as

$$x(t) = \sum_{k=1}^{M} \theta_k \phi_k(t) \tag{2.2}$$

for a particular set of basis functions $\Phi = \{\phi_k(t)\}$. The parametric model (2.2) provides a relation between estimation of the parameter values and estimation of the continuous function.

In this sense, a parametric model (2.2) transfers uncertainty evaluation on a finite-dimensional parameter space to a continuous-time function with infinitely many values and we can define the uncertainty associated with an estimate of the function $x(t)$ at a time instant t as

$$u^2(x(t)) := cov(x(t), x(t)).$$

In Section 2.4, we develop a parametrisation of the continuous function $x(t)$ based on a measurement result for the discrete-time estimate $x[n]$. In order

to assign an uncertainty to the resulting continuous-time estimate $\hat{x}(t)$, a framework for a model for the state of knowledge about a continuous function is required. In the following, we develop such a framework as a consistent extension of the framework applied for static measurements.

The proposed methodologies are based on the well-established theory of stochastic processes [20, 36–39]. We show that uncertainty evaluation on finite parameter spaces carries over consistently to a framework for continuous functions when stochastic processes are considered as a model for the state of knowledge about a deterministic function. We focus on the definition and interpretation of the stochastic processes as a state of knowledge model and define their propagation through a measurement model.

2.2 A model for the state of knowledge

For the evaluation of measurement uncertainty in the static case, knowledge about the unknown unique value of the measurand is modelled by a random variable, which is characterised by a state of knowledge probability density function (PDF). When the measurand's value depends on time so does the corresponding random variable, which results in a stochastic process; cf. [20]. Hence, uncertainty evaluation in the analysis of dynamic measurements formally requires that a stochastic process be assigned to model the knowledge about a (deterministic) continuous function. This has already been pointed out in [40, 41]. Subsequently, we extend the results of [40, 41] to a complete framework for the evaluation of uncertainty for continuous-time measurements.

Definition 2.1 (State of knowledge about a continuous function)**.** *The state of knowledge about a continuous function $x(t) \in C([a,b],\mathbb{R})$ is modelled by a continuous-time stochastic process $X_t : [a,b] \times \Omega \to \mathbb{R}$ with probability space $(\Omega, \mathcal{M}, \mathbb{P})$, such that for any set of time samples $(t_1, \ldots, t_N)$ the corresponding probability measure*

$$\nu_{\boldsymbol{x}_{1:N}}(F_1 \times \ldots \times F_N) = \mathbb{P}(X(t_1) \in F_1, \ldots, X(t_N) \in F_N)$$

models the state of knowledge about the values of $x(t)$ at these time samples.

As for the PDF calculus, the proposed model for the state of knowledge allows for the definition of an estimate of the continuous function and its associated uncertainty.

Definition 2.2 (Uncertainty of a continuous function)**.** *For the continuous function $x(t) \in C([a,b],\mathbb{R})$, consider the stochastic process $X_t : [a,b]\times\Omega \to \mathbb{R}$ modelling the state of knowledge of $x(t)$ on the finite interval $[a,b]$. Assume that $\mathbb{E}(|X(t)|) < \infty$ for all $t \in [a,b]$. The estimate of $x(t)$ is then defined as the mean function*

$$\hat{x}(t) := m_x(t) = \{\mathbb{E}(X(t)), t \in [a,b]\}. \tag{2.3}$$

Assume that $\mathbb{E}(|X(t)|^2) < \infty$ for all $t \in [a,b]$. Then the uncertainty associated with $x(t)$ is defined as the (auto-)covariance function

$$C_{X,X}(t,s) = \{cov(X(t),X(s)), t,s \in [a,b]\} \tag{2.4}$$

of the stochastic process.

According to Def. 2.1, the evaluation of the mean (2.3) and covariance function (2.4) for a finite set of time samples is equivalent to the result obtained with PDF calculus for a corresponding discretisation of the continuous function.

2.3 Evaluation of continuous-time uncertainty

In order to evaluate the uncertainties in a continuous-time estimation, a stochastic process has to be assigned to a quantity with time-varying values. For discrete-time functions, Bayesian inference can be employed to assign a corresponding state of knowledge PDF associated with the vector of function values. However, a straightforward increase of the number of time sample points in the discretisation to yield the continuous function as a limit would result in serious conceptual difficulties for a corresponding Bayesian inference. The reason is that the posterior estimate then becomes inconsistent with the true value of the measurand. There is an ongoing discussion about this inconsistency in the literature; cf. [42–46]. The bottom line is that there are types of prior knowledge for which the resulting posterior becomes inconsistent. To this end, a non-parametric Bayesian inference can be used. This class of regression methods performs a Bayesian inference on a finite set of hyper-parameters which determine an infinite-dimensional set of basis functions in the time domain. Typical examples are penalised splines [47, 48], wavelets [49, 50], (mixtures of) Dirichlet processes [51, 52] or Gaussian processes and reproducing kernel Hilbert space methods [53, 54]. A

recent overview on non-parametric Bayesian methods is given in [55], where drawbacks and limitations of the above approaches are also discussed.

Example 2.2. *Consider the model of evaluation (2.1) in Example 2.1. Assume that knowledge about the systematic correction c is available by means of a univariate PDF* $p_c(c) = \mathcal{N}(\hat{c}, \sigma_{\hat{c}}^2)$*. Knowledge about the dynamic input quantity* $y(t)$ *is assumed to be given by means of (continuous) observations modelled as*

$$w(t) = s(t) + z(t), \tag{2.5}$$

where $s(t)$ *denotes an unknown deterministic function and* $z(t)$ *denotes the realisation of an Ornstein-Uhlenbeck process with parametrised covariance function*

$$C_z(t, s) = \sigma_z^2 e^{-|t-s|/\tau},$$

where the parameters σ_z *and* τ *are assumed to be known. For any (finite) set of time sample points, application of a Bayesian inference results in a normal posterior PDF. Hence, a Gaussian process*

$$Y_t \sim GP(w(t), C_z(t, s)) \tag{2.6}$$

is associated with the dynamic input quantity.

2.3.1 PDF calculus for continuous functions

In finite dimensions, propagation of uncertainty by means of PDF calculus is carried out as a propagation of probability density functions (PDFs). We extend this concept to the treatment of continuous functions by a propagation of stochastic processes.

Stochastic process as "PDF"

The finite-dimensional probability distributions of a continuous-time stochastic process $X_t : T \times \Omega \to \mathbb{R}$ with probability space $(\Omega, \mathcal{M}, \mathbb{P})$ determine a family of probability measures of function values [56]. Thus, a stochastic process relates the measure of a probability space to a measure on a function space [37]. Therefore, a σ-algebra on a function space F is generated by the so-called cylinder sets, which for Borel sets $B \in \mathbb{R}^n$ are given by finite intersections of sets of the form [37, 56]

$$R(t_1, \ldots, t_n; B) = \{f \in F : (f(t_1), \ldots, f(t_n)) \in B\}. \tag{2.7}$$

Let $\mathcal{F}_T$ denote the smallest σ-algebra which contains all cylinder sets (2.7). A stochastic process $X_t : T \times \Omega \to \mathbb{R}$ with probability space $(\Omega, \mathcal{M}, \mathbb{P})$ encodes a mapping from the σ-algebra $\mathcal{M}$ to the σ-algebra $\mathcal{F}_T$ and hence, the inverse image of a set in $\mathcal{F}_T$ under this mapping is $\mathbb{P}$-measurable [37]. This assignment of measure on function space is called the law of the stochastic process. Evaluation of probability measure is then carried out by means of integration over sample paths of the stochastic process. Thereby, the properties of the process sample paths specify the function space of integration.

The prototype example for such a space is the classical Wiener space equipped with the so-called Wiener measure [57]. For a cylinder set

$$R(t_1, \ldots, t_n; B) = \{f \in C_0[0,1] : (f(t_1), \ldots, f(t_n)) \in B\} \tag{2.8}$$

the Wiener measure is calculated as

$$\begin{aligned} \mathbb{W}(R(t_1, \ldots, t_n; B)) = \int_B \prod_{j=1}^{n} & \frac{1}{(2\pi(t_j - t_{j-1}))^{-1/2}} \\ & \times \exp\left(-\frac{(u_j - u_{j-1})^2}{2(t_j - t_{j-1})}\right) du_1 \ldots du_n. \end{aligned} \tag{2.9}$$

Note that the evaluation of the measure $\mathbb{W}$ for a set of functions in equation (2.9) is carried out by integration over a finite-dimensional space of time samples. Evaluation of measure for infinitely many time samples is carried out by a limit process on the σ-algebra generated by the cylinder sets (2.7); cf. [57].

Let $\mathbf{x}$ denote the vector of values of $x(t) \in C([I], \mathbb{R})$ evaluated at $\{t_1, \ldots, t_n\} \subset I$. Assume that a PDF $p_{\mathbf{x}}$ is associated with $\mathbf{x}$ modelling the state of knowledge about its value. This PDF determines the probability measure

$$\nu_{\mathbf{x}}(B) = \int_B p_{\mathbf{x}}(\boldsymbol{\xi}) d\boldsymbol{\xi},$$

which denotes the probability of the corresponding simultaneous credible band for every Borel set $B \in \mathcal{B}(\mathbb{R}^n)$. Since the vector $\mathbf{x}$ is a sequence of function values $x(t_k)$, evaluation of $\nu_{\mathbf{x}}(B)$ can be interpreted as the evaluation of probability of an corresponding cylinder set (2.8). That is, $\nu_{\mathbf{x}}(B)$ may be interpreted as a cylinder set measure on the space of potential continuous-time measurand $x(t)$. In this sense, the PDF $p_{\mathbf{x}}$ determines a measure for the family of cylinder sets

$$\{R(t_1, \ldots, t_n; B) | B \in \mathcal{B}(\mathbb{R}^n)\}.$$

Considered the other way around, in this sense a cylinder set measure [37] is a consistent collection of measures, with each one corresponding to a state of knowledge PDF in line with the GUM.

In the measurement analysis for finite-dimensional measurands, credible intervals are often of interest in addition to the estimate and associated uncertainty. An extension of the concept of credible intervals to a "credible region" on the function space can be derived for continuous functions when their associated stochastic processes have continuous sample paths.

Proposition 2.1. *Let the continuous-time stochastic process* $X_t : [a,b] \times \Omega \to \mathbb{R}$ *have continuous sample paths and let* $g(t) \in C([a,b],\mathbb{R})$ *denote a continuous deterministic function on the interval* $[a,b]$*. Then* $M(\omega) := \sup_{t\in[a,b]} |X(t,\omega) - g(t)|$ *is a measurable random variable.*

Proof. The proof goes along with that of Proposition 77 in [57]. □

In practice, this can be approximately calculated as simultaneous credible intervals for a sufficiently dense discretisation or as the result of a corresponding limit process.

Propagation of stochastic processes

In finite dimensions, the PDF associated with the measurand is related to the PDF assigned to the input quantities by the change of variables formula (1.4). As noted, for instance in [37, 58], the change of variables formula does not carry over to infinite dimensions. That is, a transformation theorem in infinite dimensions is not obtained by simply considering the derivative of the considered mapping. Nevertheless, for various specific situations the corresponding propagation of stochastic processes has been investigated in the literature, e.g., [36–38, 59].

A formal extension of PDF calculus to the treatment of continuous functions is given by the following definition.

Definition 2.3 (PDF calculus for continuous functions)**.** *Consider function spaces* $V, W \subseteq C([a,b],\mathbb{R})$*. Assume that the measurand* $x \in W$ *is evaluated according to the model function*

$$x(t) = f(y(t)),$$

with input quantity $y \in V$ and operator $f : V \to W$. Assume that uncertain knowledge about $y(t)$ is modelled by an associated stochastic process Y_t with sample paths almost surely in V. Then, the state of knowledge about the measurand $x(t)$ is modelled by the stochastic process X_t with

$$\{X(t), t \in [a, b]\} = \{f(Y(t)), t \in [a, b]\}.$$

Hence, PDF calculus for continuous functions is defined as the propagation of the process' sample paths through the (deterministic) model function. In a numerical implementation this can be carried out for discrete sample paths as shown below. This means ensuring that the resulting discretisation error is negligibly small compared with the obtained uncertainty.

Remark 2.1. *Assume that the measurement model function $f(y(t))$ can be consistently applied for any finite set of time samples, i.e., the discretisation error is equal to zero. The propagation of uncertainty according to Def. 2.3 can then be carried out as the propagation of the individual members of the family of finite-dimensional probability measures*

$$\{\nu_{\mathbf{y}_{1:N}} | t_1, \ldots, t_N \in [a, b], N \in \mathbb{N}\}$$

of the stochastic process Y_t, which models the state of knowledge about $y(t)$ through the discretisations of the operator f to the corresponding family of finite-dimensional probability measures

$$\{\nu_{\mathbf{x}_{1:N}} | t_1, \ldots, t_N \in [a, b], N \in \mathbb{N}\}$$

by means of the change of variables formula.

Hence, when the discretisation error for the mapping f is equal to zero, the family of finite-dimensional distributions obtained is Kolmogorov consistent and determines the stochastic process X_t being sought. This ideal case is given in the following example. However, in practice only an approximation can be achieved.

Example 2.3. *Consider the propagation of uncertainty for the continuous-time model (2.1) with associated stochastic process (2.6) and $\mathcal{N}(\hat{c}, \sigma_{\hat{c}}^2)$ modelling the state of knowledge about the systematic correction. Since the model is linear, the stochastic process which models the state of knowledge about the measurand $x(t)$ is given by*

$$X_t \sim GP(w(t) + \hat{c}, C_z(t, s) + \sigma_c^2). \tag{2.10}$$

For one particular set of time samples $\mathbf{w} = (w(t_1), \ldots, w(t_N))$*, this corresponds to*

$$x(t_1), \ldots, x(t_N) | w(t_1), \ldots, w(t_N), \sigma_c, \sigma_z, \tau \sim \mathcal{N}(\mathbf{w} + \hat{c}, V), \tag{2.11}$$

with the covariance matrix $V_{mn} = C_z(t_m, t_n) + \sigma_{\hat{c}}^2$*. Hence, equation (2.10) encodes uncertainty propagation in terms of (2.11) for all finite sets of time samples.*

Remark 2.2. *The assumption for the function* f *in 2.1 can often be relaxed in the following way. Assume that for any family of refinements* $\mathcal{Z}_0 \subset \mathcal{Z}_1 \subset \ldots$ *of an equidistant partition of the time interval* $[a, b]$*, there exists an element* $\mathcal{Z}_n$ *such that the discretisation error for application of* f *with this partition is zero for all* $m \geq n$*. Then, for any finite set of time samples* $\{t_1, \ldots, t_N\}$*, not necessarily equidistant, there exists an element* $\mathcal{Z}_{n_0} \supseteq \{t_1, \ldots, t_N\}$ *with* $n_0 \geq n$*. Application of the change of variables formula (1.4) to* $\mathcal{Z}_{n_0}$ *and subsequent marginalisation to the set* $\{t_1, \ldots, t_N\}$ *then formally realises the propagation of uncertainty.*

In finite dimensions random variables are represented by the Radon-Nikodym derivative w.r.t. Lebesgue measure. That is, the Lebesgue measure serves as a reference measure in finite dimensions. However, the Lebesgue measure does not carry over to infinite-dimensional function spaces [58]. As a substitute, the Wiener measure is usually considered as a reference measure for infinite-dimensional function spaces. A typical example is the class of Itō diffusion processes.

Definition 2.4 (Itō stochastic process [60])**.** *A stochastic process is called an Itō process if it can be written as*

$$X_t = X(0) + \int_0^t \mu(s, X_s) ds + \int_0^t \sigma(s, X_s) dW_s, \tag{2.12}$$

where μ *and* σ *are assumed to be non-anticipating functions and* W_s *denotes a standard Brownian motion (Wiener process). The first integral in equation (2.12) is a standard Riemann integral, whereas the second is considered as Itō integral.*

Diffusion processes provide a model for a wide range of stochastic processes, and well-established techniques for the estimation of such processes exist, such as the Kalman-Bucy filter [61].

For a general continuous-time stochastic process X_t, a probability density function $p_{X_t}(x,t)$ can be determined which, for fixed t, encodes the PDF of the random variable $X_t = X(t)$. This concept is applied, for instance, in [62] to derive Bayesian posterior density functions for stochastic processes. The probability density function of a diffusion process can be obtained as a solution to the Fokker-Planck differential equation [63]:

$$\frac{\partial p_X}{\partial t}(x,t) = -\frac{\partial}{\partial x}\left(\mu(x,t)p_X(x,t)\right) + \frac{1}{2}\frac{\partial^2}{\partial x^2}\left(\sigma^2(x,t)p_X(x,t)\right).$$

The mean function $m_X(t)$ is then obtained as the expectation of the probability density function $p_X(\cdot,t)$. The covariance function $C_{XX}(t,t')$ is obtained from the probability density function as

$$C_{XX}(t,t') = \int\int (X(t) - m_X(t))(X(t') - m_X(t'))p_X(x,t,x',t')dxdx'.$$

A closed formula for the propagation of diffusion processes for a certain class of model functions is given by Itō's Lemma [60, 64]. A more general investigation on the propagation of stochastic processes through certain classes of operators can be found in [38, 65].

Propagation of general stochastic processes can be carried out by means of numerical simulations. The result is a set of *discrete* sample paths obtained by propagation of discrete sample paths of an input stochastic process through (a discretisation of) the considered measurement model. Hence, propagation of stochastic processes follows a similar scheme as the Monte Carlo integration for PDF calculus in finite dimensions. However, contrary to the application of the Monte Carlo simulation in the static case, the discretisation for the numerical propagation of stochastic process sample paths requires careful consideration of the resulting discretisation error of the applied mapping; cf. [66, 67].

$$\left\{\mathbf{y}^{(k)}(t) \sim \mathbf{Y}_t\right\}_{k=1}^{N_{MC}} \longrightarrow \boxed{\mathsf{x}^{(\mathsf{k})}(\mathsf{t}) = \mathsf{f}(\mathbf{y}^{(\mathsf{k})}(\mathsf{t}))} \longrightarrow \left\{x^{(k)}(t) \sim X_t\right\}_{k=1}^{N_{MC}}$$

An estimate of the measurand $y(t)$ and its associated uncertainty are then obtained as the mean function and the auto-covariance function from simulated sample paths. This numerical simulation represents an implementation of the formal definition for PDF calculus for continuous functions in Def. 2.3.

2.3.2 Uncertainty calculus for continuous functions

In the previous section, we extended the PDF calculus of GUM-S1 [4] to continuous-time measurements by means of the propagation of sample paths of stochastic processes. In the present section, we aim to develop a simplified application of this framework in a case, in which only an estimate and its associated uncertainty are of interest, as is done in the uncertainty calculus of GUM. This framework is exact for linear models and is based on the propagation of moments of stochastic processes through linear operators [38, 59]. This work extends the results that we presented in [41].

Proposition 2.2 (Uncertainty calculus for linear functionals)**.** *Consider that the measurand x is estimated according to a measurement model, which is described by a linear bounded functional $F : V \to \mathbb{R}, x = F\{y(t)\}$ represented as*

$$x = \int_0^T f(t)y(t)dt.$$

Assume that a stochastic process with continuous sample paths has been assigned to the continuous function $y(t) \in V = C([0,T],\mathbb{R})$ as a model for the state of knowledge about its values. Then, the estimate $\hat{x}$ of the measurand x and its associated uncertainty are given by

$$\hat{x} = \int_0^T f(t)m_y(t)dt \tag{2.13}$$

$$u^2(\hat{x}) = \int_0^T \int_0^T f(t)f(t')C_{Y,Y}(t,t')dtdt'. \tag{2.14}$$

Proof.

$$\begin{aligned}
\hat{x} =& \mathbb{E}\left\{\int_0^T f(t)Y_t dt\right\} = \int_0^T f(t)\mathbb{E}\{Y_t\}dt = \int_0^T f(t)m_y(t)dt \\
u^2(\hat{x}) =& \mathbb{E}\left\{\left(\int_0^T f(t)Y_t - f(t)m_y(t)dt\right)\left(\int_0^T f(t')Y_{t'} - f(t')m_y(t')dt'\right)\right\} \\
=& \int_0^T \int_0^T f(t)f(t')C_{Y,Y}(t,t')dtdt'.
\end{aligned}$$

□

Example 2.4. *Consider the measurand with model of evaluation (2.1) for which state of knowledge is modelled by the stochastic process (2.10). Assume*

that for the continuous-time measurand $x(t)$ the mean is to be evaluated for a finite interval:

$$\bar{x} = \mathrm{mean}_{t\in[a,b]}\, x(t).$$

Then, the estimate and its associated uncertainty for $\bar{x}$ are given by

$$\begin{aligned}\hat{\bar{x}} =& \frac{1}{b-a}\int_a^b m_x(t)dt = \hat{c} + \frac{1}{b-a}\int_a^b w(t)dt \\ u^2(\hat{\bar{x}}) =& \frac{1}{(b-a)^2}\int_a^b\int_a^b C_z(t,s)dtds + \sigma_c^2 \\ =& 2\sigma_z^2\left(\frac{\tau}{b-a} - \frac{\tau^2}{(b-a)^2}(1-e^{-(b-a)/\tau})\right) + \sigma_c^2.\end{aligned}$$

Proposition 2.3 (Equivalence to GUM uncertainty calculus)**.** *The propagation of the covariance function of a stochastic process, which models the state of knowledge about the continuous function $y(t)$ is equivalent to the application of GUM uncertainty calculus when y is not time-dependent.*

Proof. A static measurement corresponds to setting $y(t) \equiv y$ in Proposition 2.2. Then the stochastic process Y_t is also independent of time, and thus becomes a random variable. Evaluation of the integrals (2.13) and (2.14) then results in

$$\begin{aligned}\hat{x} =& \mathbb{E}\left\{Y\int_0^T f(t)dt\right\} = \hat{y}\int_0^T f(t)dt =: \hat{y}a \\ u^2(\hat{x}) =& \mathbb{E}\left\{(Y-\hat{y})^2\int_0^T\int_0^T f(t)f(t')dtdt'\right\} = u^2(\hat{y})a^2,\end{aligned}$$

which is equivalent to an application of uncertainty calculus. □

Similarly, the propagation of covariance and mean function for linear operators can be obtained.

Proposition 2.4 (Uncertainty calculus for linear operators)**.** *Consider that the continuous-time measurand $x(t) \in C([0,T],\mathbb{R})$ is estimated as*

$$x(t) = H\{y(t)\},$$

with the linear operator $H : V \to C([0,T],\mathbb{R})$ on the function space V. Assume that for the function $y(t) \in V$, the state of knowledge is modelled by the stochastic process Y_t with the mean function $m_y(t) \in V$ and covariance

function $C_{Y,Y}(t,t')$, with $C_{Y,Y}(\cdot,t') \in V$ and $C_{Y,Y}(t,\cdot) \in V$. Assume that the sample paths of Y_t belong to V almost surely.

Then, if the operator H satisfies $\mathbb{E}(|H\{Y(t,\omega)\}|) < \infty$, the estimate $\hat{x}(t)$ of the measurand $x(t)$ is given by the mean function

$$m_x(t) = H\{m_y(t)\}. \tag{2.15}$$

If the operator H satisfies $\mathbb{E}(|H(\{Y(t,\omega)\})|^2) < \infty$, the associated uncertainty is given by the covariance function

$$C_{X,X}(t,t') = H_t\{H_{t'}\{C_{Y,Y}(t,t')\}\} \tag{2.16}$$

of a stochastic process X_t.

Proof. The proof follows from the interchangeability of expectation and linear operators; cf. [20].

□

Corollary 2.1. *When H in Proposition 2.4 is a linear integral operator with operator kernel function $h(t,\tau)$, the corresponding model of evaluation is*

$$x(t) = H\{y(t)\} = \int_0^T h(t,\tau)y(\tau)d\tau. \tag{2.17}$$

Then the estimate $\hat{x}(t)$ of $x(t)$ and its associated uncertainty are given by

$$\hat{x}(t) = \int_0^T h(t,\tau)m_y(\tau)d\tau \tag{2.18}$$

$$C_{X,X}(t,t') = \int_0^T \int_0^T h(t,\tau)C_{Y,Y}(\tau,\tau')h(t',\tau')d\tau d\tau'. \tag{2.19}$$

Proof. The proof is in line with that of Proposition 2.2 due to the continuity of the kernel function. □

Note that the operator H has been assumed to be deterministic. We summarise the above results in Table 2.1.

A typical example for a linear operator is the derivative operator. The corresponding model function, the mean function and the covariance function

GUM	Extension to continuous functions
Measurand	
$\mathbf{x} \in \mathbb{R}^N$	$x(t) \in C([a,b])$
Description of knowledge	
$\mathbf{X} = (X_1, \ldots, X_N)$	$\{t \to X(t)\}$
Standard uncertainty	
$U_x = \mathrm{cov}(\mathbf{X})$	$\{t, t' \to C_{X,X}(t,t')\}$
Linear model	
$\mathbf{X} = \mathbf{H}\mathbf{Y}$	$y(t) = \int h(t,\tau) y(\tau) d\tau$
Propagation of uncertainty	
$U_{\hat{\mathbf{x}}} = H U_{\hat{\mathbf{y}}} H^T$	$C_{Y,Y}(t,t') = \int\int h(t,\tau) C_{Y,Y}(\tau,\tau') h(t',\tau') d\tau d\tau'$

Table 2.1: Relation of propagation of covariance functions to propagation of the GUM uncertainty propagation.

are then given by

$$x(t) = \frac{\partial}{\partial t} y(t) \tag{2.20}$$

$$m_x(t) = \frac{\partial}{\partial t} m_y(t) \tag{2.21}$$

$$C_{X,X}(t,t') = \frac{\partial}{\partial t}\left(\frac{\partial}{\partial t'} C_{Y,Y}(t,t')\right). \tag{2.22}$$

In this example, the assumed boundedness of the expectation in Proposition 2.4 corresponds to the condition for the interchangeability of the derivative and integral.

An example for an integral operator is the continuous Fourier transform. Its kernel function is given by $h(f,t) = \exp(-2\pi j f t)$ where $j = \sqrt{-1}$. Provided that the Fourier transform of the samples paths of the stochastic process Y_t exists almost surely, the corresponding model function, the mean function and the covariance function are given by

$$x(f) = \int_{-\infty}^{\infty} e^{-2\pi j f t} y(t) dt \tag{2.23}$$

$$m_x(f) = \int_{-\infty}^{\infty} e^{-2\pi j f t} m_y(t) dt = \mathcal{F}(m_y(t)) \tag{2.24}$$

$$C_{X,X}(f,f') = \int_{-\infty}^{\infty}\int_{-\infty}^{\infty} e^{-2\pi j f t} C_{Y,Y}(t,t') e^{-2\pi j f' t'} dt dt'. \tag{2.25}$$

Proposition 2.5 (Equivalence to GUM uncertainty calculus)**.** *The propagation of the covariance function for linear integral operators is equivalent to the GUM uncertainty calculus when a finite discretisation of the input signal $y(t)$ and the operator is considered and provided that the discretisation error is negligible.*

Proof. Let $\mathbf{y} = (y[0], \ldots, y[N])$ denote a discretisation of $y(t)$ on the interval $[0, T]$ and let

$$\mathbf{M_h} = T_s \cdot \begin{pmatrix} h(0, NT_s) & \ldots & h(0,0) \\ & \vdots & \\ h(NT_s, NT_s) & \ldots & h(NT_s, 0) \end{pmatrix}.$$

denote the matrix of the corresponding discretisation of the operator kernel function with sampling interval length T_s. Then equation (2.17) denoting the model of evaluation reduces to

$$\mathbf{x} = \mathbf{M_h y}.$$

For the application of GUM uncertainty calculus, limited knowledge about $\mathbf{y}$ is modelled by means of an estimate $\hat{\mathbf{y}}$ and its associated uncertainty (covariance matrix) $U_{\hat{\mathbf{y}}}$. The mean (2.18) and uncertainty (2.19) are then given by

$$\hat{\mathbf{x}} = \mathbf{M_h}\hat{\mathbf{y}} \tag{2.26}$$

$$U_{\hat{\mathbf{x}}} = \mathbf{M_h} U_{\hat{\mathbf{y}}} \mathbf{M_h}^T, \tag{2.27}$$

which is equivalent to the evaluation of $\hat{y}(t)$ and $C_{Y,Y}(t, t')$ at the considered time samples. □

The proposed propagation of covariance function and mean function is exact for bounded linear operators and functionals. Moreover, for Gaussian processes, this characterisation of the state of knowledge is complete. In the case of non-linear operators, the resulting process associated with the state of knowledge about the measurand is generally non-Gaussian. Then methods can be applied which approximate the measurement equation or the calculation of the process associated with the measurand. For instance, a Taylor expansion of the covariance function is used in [68] to approximate the mean and covariance function of the considered output process. In [69], variational inference is used to derive a Gaussian process, which represents an observed diffusion process, which is optimal in the sense of Kulback-Leibler

divergence. In both cases, the mean and covariance function are propagated approximately.

Here, we consider the extension of uncertainty calculus to the treatment of continuous functions based on the Frechét derivative of a non-linear operator. This results in a formula for the corresponding uncertainty evaluation scheme, which is closely related to that for the case of static measurements.

Definition 2.5 (Propagation for non-linear operators)**.** *Assume that the evaluation of the measurand $x(t) \in C([0,T],\mathbb{R}^m)$ is modelled by the operator equation*

$$x(t) = H\{y(t)\}$$

for some input quantity $y(t) \in C([0,T],\mathbb{R}^n)$ and Frechét differentiable operator H. Then the estimate $\hat{x}(t)$ of $x(t)$ and its associated uncertainty are calculated as

$$m_x(t) = \hat{x}(t) = H\{\hat{y}(t)\} \tag{2.28}$$

$$C_{X,X}(t,t') = H_{\hat{y}}\left(H_{\hat{y}} C_{Y,Y}(t,t')\right), \tag{2.29}$$

where $H_{\hat{y}}$ denotes the Frechét derivative of the operator H at $\hat{y}$.

The proposed evaluation of the estimate $\hat{x}(t)$ corresponds to that in the static case. The formula for the evaluation of uncertainty follows from Proposition 2.4 since the Frechét derivative is, by definition, a linear operator.

2.4 Discrete-time processing for continuous-time measurements

A (separable) stochastic process is (uniquely) defined by its family of finite dimensional PDFs. However, in practice, some parametric description of this family of PDFs is required in order to carry out calculations. This can be realised in terms of a set of basis functions as in Eq. (2.2) or as a stochastic differential equation as in Eq. (2.12). Here, we develop a parametrisation directly from the discrete-time analysis result. Therefore, we employ a scheme for the reconstruction of a continuous-time function from its discrete-time counterpart based on the sampling theorem of signal processing [70–72].

2.4.1 Reconstruction of continuous signals

The theoretically distortionless reconstruction of a continuous-time signal from its discretisation is ensured by the sampling theorem of signal processing [70].

Proposition 2.6 (Sampling theorem)**.** *Any continuous function $x(t)$ which consists of frequencies from 0 to some f_1 can be represented by the following series*

$$x(t) = \sum_{n=-\infty}^{\infty} x_n \frac{\sin \pi \left(2 f_1 t - n\right)}{\pi (2 f_1 t - n)}, \tag{2.30}$$

with $x_n = x(n/2f_1)$. Conversely, any function $x(t)$ that is represented by the series (2.30) only consists of frequencies from 0 to f_1.

Proof. The proof can be found, for instance, in [72] and [70]. □

Note that equation (2.30) denotes a particular interpolation of the discretisation of the continuous-time signal $x(t)$. The assumed band-limitation of $x(t)$ ensures that the interpolation error is zero.

In practice, the continuous time function may not be band-limited. The resulting interpolation error then has to be accounted for in the uncertainty budget unless its value is negligible. However, the function can often be considered to be *essentially band-limited* such that the truncation error can be expected to be negligible. This is satisfied, for instance, for functions belonging to some Schwartz space [73]. A comprehensive derivation of bounds on the truncation error can be found in [73].

2.4.2 Parametrisation by discrete-time estimate

In the following, we consider that knowledge about the continuous function $x(t)$ is available as an estimate $\hat{\mathbf{x}} = (\hat{x}[0], \ldots, \hat{x}[N-1])$ of discrete-time values for the finite time interval $[0, (N-1)T_s]$ together with an associated uncertainty. Equation (2.30) then results in the continuous-time function

$$\tilde{x}(t) = \sum_{n=0}^{N-1} x[n] sinc\left(\frac{t - nT_s}{T_s}\right), \tag{2.31}$$

where

$$sinc(t) = \begin{cases} 1 & t = 0 \\ \frac{\sin(\pi t)}{\pi t} & t \neq 0 \end{cases} .$$

denotes the cardinal sine function. Thereby, equation (2.31) relates the knowledge about the discrete-time sequence to a continuous function by means of the following proposition.

Proposition 2.7 (PDF calculus for continuous function)**.** *For the time sample points* $\{t_0, \ldots, t_{N-1}\}$ *with* $t_k = kT_s$ *and sampling interval length* T_s*, let*

$$\mathbf{x} = (x[0], \ldots, x[N-1])^T$$

denote the sequence of corresponding discrete-time function values $x[k] = x(t_k)$*. Assume that limited knowledge about these values is modelled by a PDF* $p_{\mathbf{x}}(\mathbf{x})$ *and that this PDF also accounts for discretisation and truncation errors caused by the finite number of samples from the measurand* $x(t)$*. This PDF then defines a parametrised continuous-time stochastic process, which models the state of knowledge about the continuous function* $x(t)$*.*

Proof. Consider the finite set of basis functions

$$\mathcal{S} = \left\{ sinc\left(\frac{t - kT_s}{T_s}\right), k = 0, \ldots, N-1 \right\} \tag{2.32}$$

and let

$$S(t) = (sinc(t/T_s), sinc((t - T_s)/T_s), \ldots, sinc((t - (N-1)T_s)/T_s))$$

denote the vector of corresponding functions. Define the continuous function

$$\tilde{x}(t) = S(t)^\top \mathbf{x}.$$

Then the PDF $p_{\mathbf{x}}(x[0], \ldots, x[N-1])$ determines a multivariate PDF

$$p_{\tilde{x};s_1,\ldots,s_m}(\tilde{x}(s_1), \ldots, \tilde{x}(s_m))$$

for any finite set of time samples $(s_1, \ldots, s_m)$ by

$$p_{\tilde{x};s_1,\ldots,s_m}(\eta_1,\ldots,\eta_m) = \int p_{\mathbf{x}}(\boldsymbol{\xi}) \begin{pmatrix} \delta(\eta_1 - \boldsymbol{\xi}^T S(s_1)) \\ \vdots \\ \delta(\eta_m - \boldsymbol{\xi}^T S(s_m)) \end{pmatrix} d\boldsymbol{\xi}.$$

Moreover, a time-dependent family of PDFs $p_{x,t}(\eta)$ is given by

$$p_{x,t}(\eta) = \int p_{\mathbf{x}}(\boldsymbol{\xi}) \delta(\eta - \boldsymbol{\xi}^T S(t)) d\boldsymbol{\xi}.$$

This determines a stochastic process X_t with the mean $m_x(t)$ and covariance function $C_{X,X}(t,t')$ given by

$$m_x(t) = \sum_{n=0}^{N-1} \hat{x}[n] sinc(\frac{1}{T_s}(t - nT_s)) \tag{2.33}$$

$$C_{X,X}(t,t') = \sum_{n,m=0}^{N-1} (V_{\mathbf{x}})_{n,m} sinc(\frac{1}{T_s}(t - nT_s)) sinc(\frac{1}{T_s}(t' - mT_s)) \tag{2.34}$$

$$= S(t) V_{\hat{\mathbf{x}}} S(t')^T, \tag{2.35}$$

where $\hat{x}[n]$ denotes the estimate of $x[n]$ and $V_{\hat{\mathbf{x}}}$ denotes the covariance matrix encoding the uncertainty associated with the estimate $\hat{\mathbf{x}}$. Due to the interpolation property of the chosen characterisation of $x(t)$, the set of time samples $\{0,\ldots,(N-1)T_s\}$ of this stochastic process corresponds to the measure $\nu_{\mathbf{x}}$ induced by the PDF $p_{\mathbf{x}}$. For any other $t_0 \notin \{0,\ldots,(N-1)T_s\}$ in the time interval $[0,(N-1)T_s]$, the stochastic process determines the probability measure

$$\begin{aligned} \nu_{x_0}(F_0) =& \mathbb{P}\{X(t_0) \in F_0\} \\ =& \mathbb{P}\left\{ \sum_{k=0}^{N-1} x[k] sinc\left(\frac{t - kT_s}{T_s}\right) \in F_0 \right\}, \end{aligned}$$

which is determined by

$$p_{x_0}(\xi) = \int p_{\mathbf{x}}(\boldsymbol{\eta}) \delta\left(\xi - \sum_{k=0}^{N-1} \eta_k sinc\left(\frac{t - kT_s}{T_s}\right)\right) d\boldsymbol{\eta}.$$

Hence, the stochastic process models the state of knowledge about the continuous function $x(t)$, consisting of the discrete-time sequence, its associated PDF and the basis functions. □

Hence, the uncertain knowledge about the discrete-time sequence $\mathbf{x}$ modelled by the PDF $p_{\mathbf{x}}$ determines a measure on the space of continuous functions with bandwidth not larger than $1/2T_s$.

Remark 2.3. *Any interpolation in this way determines a stochastic process. However, the set of basis functions employed here is preferred because of the following advantages:*

- *The sinc function corresponds to an ideal reconstruction of the continuous signal provided that the assumptions of the sampling theorem are satisfied.*
- *The frequency content of the interpolation result does not exceed that of the discrete-time function. Hence, the chosen basis does not introduce a bias to the estimation.*
- *The employed basis does not require additional assumptions on the continuous function.*
- *The sinc functions provide an orthonormal basis on $L^2(\mathbb{R})$.*
- *The sinc functions are elements of $C^\infty(\mathbb{R})$.*
- *Extending an existing parametrisation of the continuous function by additional discrete-time values does not require recalculation the basis functions used or the expansion coefficients.*

Any interpolation has an impact on the corresponding frequency content of the continuous function. The basis of sinc functions employed here represents the case of an ideal low pass filter [13, 74]. Hence, the resulting continuous-time function does not contain frequency content beyond the sampling frequency. Consequently, if the sampling rate in the measurement analysis is too small, the interpolation result does not correspond to the actual measurand, but still reflects the knowledge obtained from the discretisation. Moreover, if the chosen sampling interval length T_s is known to result in a significant discretisation error, it would have to be accounted for in the uncertainty budget for the discrete-time estimate as well.

2.4.3 Propagation of uncertainty

Propagation of uncertainty for a parametrised stochastic process can be performed very efficiently. Let $x(t)$ denote a continuous function with parametri-

sation

$$x(t) = \sum_{k=1}^{N} \theta_k \phi_k(t), \tag{2.36}$$

where knowledge about the parameters is modelled by an associated PDF $p_\theta(\boldsymbol{\theta})$. Then the stochastic process X_t, which models the state of knowledge about the values of the continuous function $x(t)$, has time-dependent probability density function

$$p_{X_t,t}(\xi) = \int p_\theta(\boldsymbol{\theta}) \delta(\xi - \boldsymbol{\theta}^T \Phi(t)) d\boldsymbol{\theta},$$

where $\Phi(t) = (\phi_1(t), \ldots, \phi_N(t))^T$.

Proposition 2.8. *Assume the continuous function $x(t)$ is expressed by equation (2.36). Consider that a linear operator $H : C(\mathbb{R}) \to C(\mathbb{R})$ is applied to the continuous function, resulting in*

$$y(t) = H\{x(t)\}.$$

Then, the mean function and the covariance function of the stochastic process Y_t which models the state of knowledge about $y(t)$ are given by

$$m_y(t) = \hat{\boldsymbol{\theta}}^T H\{\Phi(t)\} \tag{2.37}$$

$$C_{Y,Y}(t,t') = H\{\Phi(t)\}^T U_{\hat{\boldsymbol{\theta}}} H\{\Phi(t')\}, \tag{2.38}$$

where $H\{\Phi(t)\} = (H\{\phi_1(t)\}, \ldots, H\{\phi_N(t)\})^T$ and $U_{\hat{\boldsymbol{\theta}}}$ denotes the matrix of mutual uncertainties $u(\hat{\theta}_k, \hat{\theta}_l)$.

Proof. The proof follows directly from the linearity of the operator and the finite decomposition (2.36) of $x(t)$. Calculation of mean function and covariance function is carried out as

$$\begin{aligned} m_y(t) =& \boldsymbol{\phi}(t)^T \int \boldsymbol{\theta} p_{\boldsymbol{\theta}}(\boldsymbol{\theta}) d\boldsymbol{\theta} = \boldsymbol{\phi}(t)^T \hat{\boldsymbol{\theta}} \\ C_{Y,Y}(t,t') =& \int (\boldsymbol{\theta}^T \Phi(t) - \hat{\boldsymbol{\theta}}^T \Phi(t))(\boldsymbol{\theta}^T \Phi(t) - \hat{\boldsymbol{\theta}}^T \Phi(t)) p_{\boldsymbol{\theta}}(\boldsymbol{\theta}) d\boldsymbol{\theta} \\ =& \Phi(t)^T U_{\hat{\boldsymbol{\theta}}} \Phi(t), \end{aligned}$$

where $\Phi(t) = (\phi_1(t), \ldots, \phi_N(t))^T$. □

Implementation of PDF calculus by means of simulations can be carried out very efficiently. Therefore, samples are drawn from the multivariate PDF associated with $\boldsymbol{\theta}$. Each sample then determines a sample path of the stochastic process associated with $y(t)$.

Example 2.5. *Consider as basis functions the set (2.32) with parameters given by the discrete-time sequence $x[0], \ldots, x[N-1]$ for $t_k = kT_s$ with sampling interval length T_s. As an operator consider the derivative*

$$y(t) = \frac{\partial x}{\partial t}(t).$$

Then, with $x(t) = \mathbf{x}^T S(t)$ and PDF $p_{\mathbf{x}}(\mathbf{x})$, the mean function and covariance function of the stochastic process Y_t which models the state of knowledge about $y(t)$ are given by

$$\begin{aligned} m_y(t) &= \sum_{k=0}^{N-1} \hat{x}[k] \frac{\partial}{\partial t} sinc\left(\frac{t - kT_s}{T_s}\right) \\ C_{Y,Y}(t,t') &= \left(\frac{\partial}{\partial t} S(t)\right)^T V_{\mathbf{x}} \frac{\partial}{\partial t} S(t'), \end{aligned}$$

with

$$\begin{aligned} \frac{\partial}{\partial t} sinc\,(z) =& \frac{\pi}{T_s} \frac{\cos(\pi z)\pi z - \sin(\pi z)}{(\pi z^2} \\ \left(\frac{\partial}{\partial t} S(t)\right)^{\top} =& \left(\frac{\partial}{\partial t} sinc(t/T_s), \ldots, \frac{\partial}{\partial t} sinc((t - NT_s)/T_s)]\right). \end{aligned}$$

where $z = (t - kT_s)/T_s$. Hence, the stochastic process Y_t is determined by the same multivariate PDF $p_{\mathbf{x}}$ as the process X_t, but with a different set of basis functions.

Remark 2.4. *In general, the evaluation of measurement uncertainty for continuous functions based on the framework presented here requires consideration of stochastic differential equations (SDEs). However, with the proposed characterisation of the stochastic process in terms of a finite function basis, the application and solution of SDEs can be avoided for the analysis of dynamic measurements.*

Chapter 3

Discrete-time analysis of dynamic measurements

In the previous chapter, we derived an assignment of a continuous-time stochastic process to the continuous-time measurand by employing a discrete-time estimate as a particular parametrisation. The goal of the present chapter is the estimation of a discrete-time variant of the measurand as a solution to the discrete-time deconvolution problem. Note that in Chapter 2 we focused on the propagation of uncertainties. That is, we did not specify any particular estimation method. Hence, regularisation in the estimation of the continuous-time measurand has not been considered. In the present chapter, we present a practical estimation procedure, which addresses regularisation for the discrete-time estimation.

3.1 Problem specification

Assume that the measurement system output signal $\mathbf{y} = (y[1], \ldots, y[N])$ can be modelled by

$$y[n] = Y[n] + \varepsilon[n] = (h_{\mathbf{\Gamma}} * X)[n] + \varepsilon[n], n = 1, \ldots, N \tag{3.1}$$

where "$*$" denotes convolution, $h_{\mathbf{\Gamma}}$ denotes the impulse response of the measurement system and $\varepsilon[n]$. The goal is to estimate $X[n]$ for $n = 1, \ldots, N$ by means of digital filtering. Therefore, a deconvolution filter is designed

w.r.t. the (uncertain) knowledge about the measurement system. The uncertainty associated with the filter parameters is evaluated by a propagation of the uncertainty associated with the knowledge about the measurement system through the filter design algorithm. We assume that the noise process is zero-mean stationary and can be modelled by an auto-regressive process of order (p, q):

$$\varepsilon[n] = \sum_{k=1}^{\min(p,n-1)} \varphi_k \varepsilon[n-k] + \sum_{k=1}^{\min(q,n-1)} \vartheta_k w[n-k] + w[n], \tag{3.2}$$

with known parameters $\varphi_1, \ldots, \varphi_p, \vartheta_1, \ldots, \vartheta_q$ and zero-mean Gaussian process $w[n] \sim \mathcal{N}(0, \sigma^2)$ with variance σ^2. From the parameters of the auto-regressive process, the covariance matrix V_ε for the noise process for the considered time instants can be calculated [60].

For the assignment of uncertainty to the observed system outputs $y[n]$, we use Bayes theorem with non-informative priors resulting in the joint PDF $\mathcal{N}(\mathbf{y}, V_\varepsilon)$, where $\mathbf{y} = (y[1], \ldots, y[N])$.

The model for the evaluation of the measurand is given by a convolution of the discrete-time sequence of observations with the deconvolution filter:

$$X[n] = \widetilde{X}[n] + \Delta[n], \tag{3.3}$$

$$\widetilde{X}[n] = \sum_{k=0}^{N_b} B_k Y[n-k] - \sum_{k=1}^{N_a} A_k \widetilde{X}[n-k], \tag{3.4}$$

where $\boldsymbol{M} = (A_1, \ldots, A_{N_a}, B_0, \ldots, B_{N_b})$ are the coefficients defining the deconvolution filter $g_{\boldsymbol{M}}(z)$, and $\Delta[n]$ denotes a systematic correction to account for the systematic error introduced by the application of the deconvolution filter 3.4. We assume that $Y[m] = 0$ for all $m < 0$.

For a finite length impulse response (FIR) filter equation (3.3) reduces to

$$\widetilde{X}[n] = \sum_{k=0}^{N_b} B_k Y[n-k], \tag{FIR-1}$$

with N_g representing the filter order of g.

For the application of infinite impulse response (IIR) filters, instead of (3.3), the recursive model (1.12) or the state-space representation (1.9) of the filter

can be considered. The corresponding model function is then given by

$$\mathbf{z}[n+1] = \mathbf{A}\mathbf{z}[n] + \mathbf{b}Y[n] \tag{IIR-1a}$$

$$\widetilde{X}[n] = \mathbf{c}^T\mathbf{z}[n] + b_0 Y[n]. \tag{IIR-1b}$$

The evaluation of uncertainty associated with the estimate (3.3) is carried out by a propagation of the uncertainty associated with the deconvolution filter coefficients and the observed output signal sequence through the measurement model.

In the following, we first focus on the evaluation of uncertainty when the contribution of the systematic error $\Delta[n]$ is negligible. In Section 3.5, we then derive a procedure to account for its contribution for a particular type of prior knowledge about the measurand.

3.2 Design of deconvolution filters

As a generalisation of the classic approaches (1.13) and (1.14) for regularised deconvolution, we consider a deconvolution filter as a cascade of a compensation filter and a low pass filter

$$g(z) = g_{comp}(z)g_{low}(z).$$

The low pass filter encodes the regularisation of the ill-posed deconvolution problem and the compensation filter approximates the reciprocal measurement system within a certain frequency region.

Design of a low pass filter is well established in the signal processing literature, see [13]. The design of a compensation filter is more difficult owing to the fact that the inverse measurement system is usually unstable. To this end, various methods can be found in the literature. In a recent comparison study, we assessed the performance and compensation quality of deconvolution filters designed using a least squares approximation in the frequency domain to those obtained by an adjustment of a z-domain rational function [15]. We found that the compensation quality of the deconvolution filters obtained depends on the type of the knowledge available about the measurement system used for the design of the filter. For instance, when knowledge is available by means of a set of frequency response values, design of an FIR filter by means of least squares was found to be superior, whereas a time reversal

method may be preferred when the measurement system is given by means of a discrete-time model; cf. [15].

In general, the design of the compensation filter can be described as a mapping $\boldsymbol{\Gamma} \mapsto f(\boldsymbol{\Gamma}) = \boldsymbol{M}$ from the parameter vector $\boldsymbol{\Gamma}$ of the measurement system to the vector $\boldsymbol{M}$ of compensation filter coefficients. The mapping is implicitly determined by the way the deconvolution filter is constructed. The parameter vector $\boldsymbol{\Gamma}$ can be the coefficients of the rational discrete or continuous time system transfer function or a vector of frequency response values.

We assume that an estimate of the measurement system parameters $\boldsymbol{\Gamma}$ has been obtained in a dynamic calibration together with a corresponding evaluation of uncertainty (e.g., [26] for the calibration of an accelerometer. The uncertainty associated with the compensation filter is then evaluated by a propagation of the uncertainty associated with $\boldsymbol{\Gamma}$ through the design method f by means of PDF calculus or uncertainty calculus, see Section 1.1.

Remark 3.1. *Throughout the next section we assume that the regularisation error $\Delta[n]$ is negligibly small. The reason is that its uncertainty contribution depends on the type of prior knowledge about the measurand, whereas that of the deconvolution filter coefficients is of generic character. In Section 3.5, we then develop a method to account for the uncertainty contribution of the regularisation error for a particular type of prior knowledge.*

3.3 Uncertainty calculus for digital filtering

The dynamic system corresponding to the digital filter is linear in its inputs and in the case of an FIR filter linear in its parameters (filter coefficients). However, model (3.3) depends non-linearly on the input quantities, and thus application of uncertainty calculus for the evaluation of uncertainty requires a linearisation; cf. [17].

Proposition 3.1 (Uncertainty calculus for digital filtering)**.** *Consider as measurand the value $X[n]$ and the discrete-time model of evaluation (3.3) with input quantities $\boldsymbol{M}$ and $\mathbf{Y}$, where for an FIR filter*

$$\boldsymbol{M} = \mathbf{g} = (g[1], \ldots, g[N_g]) \tag{3.5}$$

$$\mathbf{Y} = (Y[n - N_g], \ldots, Y[n]), \tag{3.6}$$

and for an IIR filter

$$\boldsymbol{M} =(a_1, \ldots, a_{N_a}, b_0, \ldots, b_{N_b}) \tag{3.7}$$
$$\mathbf{Y} =(Y[1], \ldots, Y[n]), \tag{3.8}$$

for which limited knowledge is available by means of an estimate $\hat{\mathbf{y}}$ *and* $\hat{\boldsymbol{\mu}}$ *with associated uncertainty given by the matrices* $(U_{\hat{\mathbf{y}}})_{k,l} = cov(\hat{y}[k], \hat{y}[l])$ *and* $U_{\hat{\boldsymbol{\mu}}}$*, respectively. Assume that the estimates of the input quantities* $\mathbf{Y}$ *and* $\boldsymbol{M}$ *have been obtained independently. Then the application of* uncertainty calculus *results in an estimate of the value of the measurand and its associated squared uncertainty which for a FIR filter is given by*

$$\hat{x}[n] =(\hat{g} * \hat{y})[n] \tag{FIR}$$
$$u^2(\hat{x}[n]) =\hat{\mathbf{y}}^T U_{\hat{\boldsymbol{g}}} \hat{\mathbf{y}} + \hat{\mathbf{g}}^T U_{\hat{\mathbf{y}}} \hat{\mathbf{g}}, \tag{FIR}$$

where

$$(U_{\hat{\mathbf{y}}})_{k,l} = cov(\hat{y}[n - N_g + k], \hat{y}[n - N_g + l]). \tag{3.9}$$

For an IIR filter, using the state-space approach [17], the corresponding result is given by

$$\hat{x}[n] =\hat{\mathbf{c}}^T \hat{\mathbf{z}}[n] + \hat{b}_0 \hat{y}[n] \tag{IIR}$$
$$u^2(\hat{x}[n]) =\phi^T(n) U_{\hat{\boldsymbol{\mu}}} \phi(n) + \hat{\mathbf{c}}^T \mathbf{P}_z(n) \hat{\mathbf{c}} + \hat{b}_0^2, \tag{IIR}$$

where

$$\boldsymbol{\phi}(n) = \left(\frac{\partial x[n]}{\partial \mu_1}, \ldots, \frac{\partial x[n]}{\partial \mu_{N+N_a+N_b+1}} \right)^T$$
$$\mathbf{P}_{\mathbf{z}}(n) = \sum_{m<n} \left(\frac{\partial \mathbf{z}[n]}{\partial y[m]} \right) \left(\frac{\partial \mathbf{z}[n]}{\partial y[m]} \right)^T u^2(\hat{y}[m]).$$

Proof. The proof for the IIR filter result is given in [17]. The formula for the FIR filter is stated without proof in [40]. A proof is given here.

The model function for the application of an FIR filter is given by

$$X[n] = f(g_0, \ldots, g_{N_g}, Y_{n-N_g}, \ldots, Y_n) = \sum_{k=0}^{N_g} g[k] Y[n-k].$$

The model input quantities are $\mathbf{g}$ and $\mathbf{Y}$ for which estimates $\hat{\mathbf{g}}$, $\hat{\mathbf{y}}$ and associated uncertainties $U_{\hat{\mathbf{g}}}$, $U_{\hat{\mathbf{y}}}$ are available by assumption. Linearisation of

the model w.r.t. to the input quantities and application of the uncertainty calculus formula (1.6) then results in

$$\begin{aligned} u^2(\hat{x}[n]) =& \sum_{k,l=0}^{N_g} \left(\frac{\partial f}{\partial g_k}\right)\left(\frac{\partial f}{\partial g_l}\right) u(g_k, g_l) + \sum_{k,l=0}^{N_g} \left(\frac{\partial f}{\partial y_{n-k}}\right)\left(\frac{\partial f}{\partial y_{n-l}}\right) u(y_{n-k}, y_{n-l}) \\ =& \sum_{k,l=0}^{N_g} \hat{y}_{n-k}\hat{y}_{n-l} u(g_k, g_l) + \sum_{k,l=0}^{N_g} \hat{g}_k \hat{g}_l u(y_{n-k}, y_{n-l}) \\ =& \hat{\mathbf{y}}_n^T U_{\hat{\mathbf{g}}} \hat{\mathbf{y}}_n + \hat{\mathbf{g}}^T U_{\hat{\mathbf{y}}_n} \hat{\mathbf{g}}. \end{aligned}$$

□

For a static signal y, the above formulas coincide with those for static measurements. For instance, for the application of an FIR filtering, the equations for the calculation of an estimate $\hat{x}[n]$ and its associated uncertainty $u^2(\hat{x}[n])$ then reduce to

$$\hat{x}[n] = \hat{y} \sum_{k=0}^{N_g} \hat{g}[k] \tag{3.10}$$

$$u^2(\hat{x}[n]) = \hat{y}^2 \mathbf{1}^T U_{\hat{g}} \mathbf{1} + u^2(\hat{y}) \sum_{k=0}^{N_g} \hat{g}^2[k] \tag{3.11}$$

$$= \hat{y}^2 \sum_{k,l=0}^{N_g} u(\hat{g}[k], \hat{g}[l]) + u^2(\hat{y}) \sum_{k=0}^{N_g} \hat{g}^2[k], \tag{3.12}$$

where $\mathbf{1}^T = (1, \ldots, 1)$, in which the entries for the $N_g + 1$ dimensional vector are equal to one. Hence, the uncertainty calculus results presented here consistently extend the methodologies applied for static measurements consistently to dynamic measurements.

3.4 PDF calculus for digital filtering

The evaluation of uncertainty by means of PDF calculus for model (3.3) is based on the propagation of the (joint) probability density function (PDF) associated with $(\mathbf{Y}, \boldsymbol{M})$ to a PDF associated with the measurand.

Proposition 3.2 (PDF calculus for digital filtering)**.** *Consider as measurand the value $X[n]$ for some time instant n and as model function the discrete-time convolution (FIR-1) and (IIR-1b), respectively, with input quantities $\boldsymbol{M}$ and $\mathbf{Y}$, where for a FIR filter*

$$\boldsymbol{M} = \mathbf{g} = (g[0], \ldots, g[N_g]) \tag{3.13}$$
$$\mathbf{Y} = (Y[n - N_g], \ldots, Y[n]), \tag{3.14}$$

and for an IIR filter

$$\boldsymbol{M} = (a_1, \ldots, a_{N_a}, b_0, \ldots, b_{N_b}) \tag{3.15}$$
$$\mathbf{Y} = (Y[1], \ldots, Y[n]), \tag{3.16}$$

for which limited knowledge is available by means of an associated (joint) PDF $p_{\mathbf{y},\boldsymbol{\mu}}$. Then the application of PDF calculus results in the PDF

$$p_{\hat{x}[n]}(\xi) = \int p_{\boldsymbol{\mu},\mathbf{y}}(\boldsymbol{\mu}, \boldsymbol{\eta}) \delta\left(\xi - (g_{\boldsymbol{\mu}} * \boldsymbol{\eta})[n]\right) d\boldsymbol{\mu} d\boldsymbol{\eta}. \tag{3.17}$$

where $\boldsymbol{\eta} = (\eta_1, \ldots, \eta_M)$.

Proof. This directly results from inserting the filter equation as model function in the PDF calculus formula. □

An extension of this result to an estimate of the measurand $\mathbf{x}$ is easily obtained by considering the multivariate distributions instead.

For FIR filters, the calculation of expectation and variance can be carried out analytically [40].

Proposition 3.3 (PDF calculus for application of FIR filters)**.** *Under the same assumptions as in Proposition 3.1, the PDF calculus result for the estimate and its associated uncertainty of the measurand X for the model (3.3) is given by*

$$\hat{x}[n] = (\hat{g} * \hat{y})[n] \tag{3.18}$$
$$u(\hat{x}[n], \hat{x}[m]) = \hat{\mathbf{g}}^T U_{\hat{\mathbf{y}}_n, \hat{\mathbf{y}}_m} \hat{\mathbf{g}} + \hat{\mathbf{y}}_n^T U_{\hat{\mathbf{g}}} \hat{\mathbf{y}}_m + Tr(U_{\hat{\mathbf{g}}} U_{\hat{\mathbf{y}}_n, \hat{\mathbf{y}}_m}), \tag{3.19}$$

where Tr denotes the trace of a matrix and $\mathbf{y}_n = (y[n], y[n-1], \ldots, y[n - N_g])^\top$.

Proof. The proof can be found in [16]. □

Note that the PDF calculus result for the case of an FIR filter differs from that of uncertainty calculus by the trace term. This difference is due to the non-linearity of the model function and can usually be expected to be small.

3.4.1 Implementation of PDF calculus

An analytical evaluation of the integral (3.17) is hardly tractable. To this end, Monte Carlo methods can be applied as a numerical solution. However, the input and output quantities in a dynamic measurement analysis are multivariate and generally high dimensional. Thus, performing Monte Carlo simulations for the implementation of PDF calculus is usually very computationally intensive. In fact, application of PDF calculus by Monte Carlo with reasonable accuracy is almost impossible on most computers due to memory issues. Hence, there is a need for efficient methods to implement PDF calculus for dynamic measurements. To this end, we develop an approach which employs the sequential character of the measurement equation [75] to allow for a memory-efficient implementation.

We consider three strategies for the implementation of a Monte Carlo method for model (3.3), which we call *Batch Monte Carlo* (BMC), *Update Monte Carlo* (UMC) and *Sequential Monte Carlo* (SMC) propagation [75]. The BMC method is a direct implementation of the PDF calculus Monte Carlo scheme described in Chapter 1. The UMC method is based on update formulas for mean and (co-) variance and described in [75]. The SMC method is related to Sequential or Particle Monte Carlo *filtering* methods [76]. In each iteration it considers propagation of the PDF associated with $y[n]$ for a particular instant n through a state-space representation of equation (3.3).

The computational expense for the uncertainty propagation for the whole sequence $\mathbf{x} = (x[1], \ldots, x[N])$ is similar for all methods. However, the required memory to calculate mean, variances and point-wise credible intervals is different. In fact, the straightforward application of BMC may be impossible for large signal sequences owing to memory issues.

Batch Monte Carlo

Assume the measurand is evaluated by means of the discrete convolution (3.3). For the evaluation of the multivariate PDF $p_{\mathbf{x}}$, samples $\mathbf{y}^{(k)}$ are drawn from

the PDF $p_{\mathbf{y}}$ associated with the input signal sequence $\mathbf{y}$ and from the PDF $p_{\boldsymbol{\mu}}(\boldsymbol{\mu})$ associated with the coefficients of the digital filter $g_{\boldsymbol{\mu}}$. These samples are then propagated through equation (3.3) as depicted in Fig. 3.1.

$$\left\{ \begin{array}{l} \mathbf{y}^{(k)} \sim p_{\mathbf{y}}(\mathbf{y}) \\ \boldsymbol{\mu}^{(k)} \sim p_{\boldsymbol{\mu}}(\boldsymbol{\mu}) \end{array} \right\}_{k=1,\ldots,K} \longrightarrow \boxed{\mathbf{x} = (\mathbf{g}_{\boldsymbol{\mu}} * \mathbf{y})} \longrightarrow \{\mathbf{x}^{(k)}\}_{k=1,\ldots,K}$$

Figure 3.1: PDF calculus for digital filtering by means of Batch Monte Carlo simulation

Carrying out the Monte Carlo scheme as in Fig. 3.1 results in sample draws from the multivariate distribution which models the state of knowledge about $\mathbf{X} = (X[1], \ldots, X[N])$. The estimate $\hat{\mathbf{x}}$ and its associated uncertainty are then calculated as mean vector and covariance matrix of the samples

$$\hat{\mathbf{x}} = \text{mean}\{\mathbf{x}^{(k)}\}_{k=1,\ldots,K} \tag{3.20}$$

$$U_{\hat{\mathbf{x}}} = \text{cov}\{\mathbf{x}^{(k)}\}_{k=1,\ldots,K}, \tag{3.21}$$

which coincides approximately with the corresponding statistics of the PDF $p_{\mathbf{x}}$, provided that K is sufficiently large. The resulting samples also allow for a computation of (point-wise) credible intervals $[x_{low}, x_{high}]$ for some prescribed coverage probability P (e.g., 95%)

$$P = \int_{x_{low}[n]}^{x_{high}[n]} p_{x[n]}(\eta) d\eta.$$

We outline the BMC method in Algorithm 1 where CalcCred denotes the calculation of point-wise credible intervals from the resulting samples; cf. [4].

Note that drawing from the multivariate PDF in line 3 can be replaced by a sequential approach employing the sequential character of the auto-regressive noise process (see (3.2) and [75]).

Application of Batch Monte Carlo requires drawing and storing samples from the multivariate PDF associated with $\mathbf{y}$ and storing the resulting samples from $p_{\mathbf{x}}$. Hence, for long signal sequences (e.g., larger than 2000), application of BMC on standard personal computers may require various adaptations of Algorithm 1 owing to the limited size of matrices which can be held in the memory.

Remark 3.2. *The suggested number of trials in [4] is given for the estimation of a univariate quantity. A reliable two-stage method to achieve a prescribed accuracy is given in [77]. For the choice of an appropriate number of Monte Carlo trials for dynamic measurement analysis we suggest considering some*

Algorithm 1: BMC: Batch Monte Carlo for PDF calculus

Initialize: set K as the number of Monte Carlo trials;
for $k = 1$ **to** K **do**
  draw $\mathbf{y}^{(k)}$ from $\mathcal{N}(\mathbf{y}, V_\varepsilon)$;
  draw $\boldsymbol{\mu}^{(k)} = (a_1^{(k)}, \ldots, a_{N_a}^{(k)}, b_0^{(k)}, \ldots, b_{N_b}^{(k)})$ from $p_{\mathbf{M}}(\boldsymbol{\mu})$;
  $\mathbf{x}^{(k)} = (g_{\boldsymbol{\mu}^{(k)}} * \mathbf{y}^{(k)})$
end
$\widehat{\mathbf{x}} = \frac{1}{K} \sum_{k=1}^{K} \mathbf{x}^{(k)}$;
$\mathbf{U}_{\widehat{\mathbf{x}}} = \frac{1}{K-1} \sum_{k=1}^{K} (\mathbf{x}^{(k)} - \mathbf{x})(\mathbf{x}^{(k)} - \mathbf{x})^\top$;
for $n = 1$ **to** N **do**
  $\mathbf{I}_{X[n]} = \texttt{CalcCred}(\{x^{(k)}[n], k = 1, \ldots, K\})$;
end

univariate measure for the remaining randomness. For instance, one may repeat the BMC method with the same number of trials several times and evaluate the maximal standard deviation of the sample means obtained over the considered time interval. The number of Monte Carlo trials needed for stabilisation of this measure should then be selected.

Sequential Monte Carlo propagation

The methodology is related to Sequential Monte Carlo *filtering* methods for the implementation of state-space estimation by Kalman filtering for non-linear systems and non-Gaussian noise [76]. The main idea of these Sequential Monte Carlo methods is to propagate initially drawn samples (particles) of the (state equation) noise process through the state-space equation to *predict* the system output. As for the classical Kalman filter, this prediction is then corrected by the actual observation of the system output; cf. [76].

Using this idea, we develop an implementation of PDF calculus Monte Carlo simulation to *propagate* uncertainty through the filtering equation sequentially. Unlike to the particle filtering, no re-weighting scheme is necessary since a propagation is being sought, not a prediction. Hence, the resulting sample draws from the PDF associated with the measurand are *independent*, which is generally not the case for Particle Filtering [76].

The initially drawn samples $y^{(k)}[1]$ from the PDF associated with $y[1]$ are propagated through the K realisations of the digital filter *simultaneously*.

Hence, at each time sample point n for all realisations of the filter coefficients, the calculation of the corresponding filter output $x^{(k)}[n]$ at this time instant is carried out. The obtained set of sample draws is of the same size for Batch Monte Carlo and Sequential Monte Carlo. However, its generation is different. When the set of samples is considered as a matrix, such as $\mathcal{M}_x$, BMC generates this matrix row-wise, whereas SMC generates it column-wise. However, the SMC algorithm can be considered to be superior only when point-wise statistics such as point-wise credible intervals are considered; cf. [75]. The reason is that their calculation only requires the individual columns of $\mathcal{M}_x$. In this case, application of BMC requires storing the $N(K+2)+N_b+N_a+1$ array elements opposed to the $K(2N_a+2_Nb+4)$ array elements for the SMC method applied to the state-space representation (1.9) to calculate these statistics, e.g., [75]. An algorithmic outline of the SMC method is given in Algorithm 2. For an efficient implementation in MATLAB see [75].

In Fig. 3.2, the required computation time on a standard Intel Core i7 with 3.4 GHz and 4 GB RAM is shown for different signal sequence lengths. Therefore, a simple example of propagation through a 6^{th} order IIR filter is considered. We increased the number of the subsequent time samples of the estimates for which mean $\hat{x}[n]$, uncertainty $u^2(x[n])$ and point-wise credible intervals $[x_l[n], x_u[n]]$ are calculated. The Batch Monte Carlo method is faster, but breaks down for large signal lengths owing to memory issues. It is worth noting that we encountered the same memory problem when trying $1.2 \cdot 10^6$ Monte Carlo runs for the analysis of a signal with 3000 samples on a UNIX work station computer with 24 cores and 96 GB of RAM. However, using the SMC method, the same calculations can be carried out on a desktop computer without any difficulty.

The drawback of the sequential approach is that it is efficient only for point-wise statistics. However, covariances, for instance, are important when subsequent to the estimation of $\mathbf{x}$ some operator or function is applied to it. If such an operator can also be evaluated sequentially, the SMC algorithm can easily be adapted to include this evaluation [75]. For example, an approximate calculation of the integral of the measurand using the trapezoidal rule

$$\int_0^{(N-1)T_s} x(t)\mathrm{d}t \approx \frac{T_s}{2}\sum_{n=1}^{N-1}(X[n]+X[n+1]) \equiv F, \tag{3.22}$$

can be carried out sequentially as follows:

1. Set $F^{(k)} = 0$ for $k = 1, \ldots, K$;

2. Calculate sequentially, starting from $n = 2$:

$$F^{(k)} := F^{(k)} + \frac{T_s}{2}(x^{(k)}[n] + x^{(k)}[n-1]).$$

The resulting set of values $F^{(k)},\ k = 1, \ldots, K$, of the (approximate) integral F can be used to calculate an estimate of F, the associated standard uncertainty and a credible interval for F. In this way, correlations and non-linear dependencies between estimates at different time instants are implicitly taken into account.

According to the Riesz representation theorem, all continuous linear functionals on the space of square-integrable functions can be written in terms of an integral as

$$\phi(x) = \int f(t)x(t)dt,$$

where the function $f(t)$ is uniquely determined by ϕ. Hence, the sequential approach allows for an evaluation of all continuous linear functionals and integral operators acting on the dynamic measurand. In this way, the impact of the limitation to point-wise statistics is reduced.

Algorithm 2: SMC: Sequential Monte Carlo for PDF calculus

Initialize: Set K as the number of Monte Carlo trials;
for $k = 1$ **to** K **do**
  draw $\boldsymbol{\mu}^{(k)} = (a_1^{(k)}, \ldots, b_{N_b}^{(k)})^\top$ from $p_{\mathbf{M}}(\boldsymbol{\mu})$;
  $d_j^{(k)} = b_j^{(k)} - b_0^{(k)} a_j^{(k)}, \quad j = 1, \ldots, N_b$;
  draw $w^{(k)}[1]$ from $\mathcal{N}(0, \sigma^2)$;
  $\varepsilon^{(k)}[1] = w^{(k)}[1]$ and $y^{(k)} = y[1] + \varepsilon^{(k)}[1]$;
  $x^{(k)}[1] = b_0^{(k)} y^{(k)}$;
  $z_j^{(k)} = 0, \quad j = 1, \ldots, N_a$;
end
$\widehat{x}[1] = \frac{1}{K} \sum_{k=1}^{K} x^{(k)}[1]$;
$u^2(\widehat{x}[1]) = \frac{1}{K-1} \sum_{k=1}^{K} (x^{(k)}[1] - \widehat{x}[1])^2$;
$\mathbf{I}_{Y[1]} = \texttt{CalcCredS}(\{x^{(k)}[1]\})$;
for $n = 2$ **to** N **do**
  for $k = 1$ **to** K **do**
    draw $w^{(k)}[n]$ from $\mathcal{N}(0, \sigma^2)$;
    $\varepsilon^{(k)}[n] =$
    $\sum_{j=1}^{\min(p,n-1)} \varphi_j \varepsilon^{(k)}[n-j] + \sum_{j=1}^{\min(q,n-1)} \vartheta_j w^{(k)}[n-j] + w^{(k)}[n]$;
    $y^{(k)} = y[n] + \varepsilon^{(k)}[n]$;
    $x^{(k)}[n] = (\mathbf{z}^{(k)})^\top \mathbf{d}^{(k)} + b_0^{(k)} y^{(k)}$;
    $z_1^{(k)} = -(\mathbf{z}^{(k)})^\top \mathbf{a}^{(k)} + y^{(k)}$;
    $z_j^{(k)} = z_{j-1}^{(k)}, \quad j = 2, \ldots, N_a - 1$;
  end
  $\widehat{x}[n] = \frac{1}{K} \sum_{k=1}^{K} x^{(k)}[n]$;
  $u^2(\widehat{x}[n]) = \frac{1}{K-1} \sum_{k=1}^{K} (x^{(k)}[n] - \widehat{x}[n])^2$;
  $\mathbf{I}_{X[n]} = \texttt{CalcCredS}(\{x^{(k)}[n], k = 1, \ldots, K\})$;
end

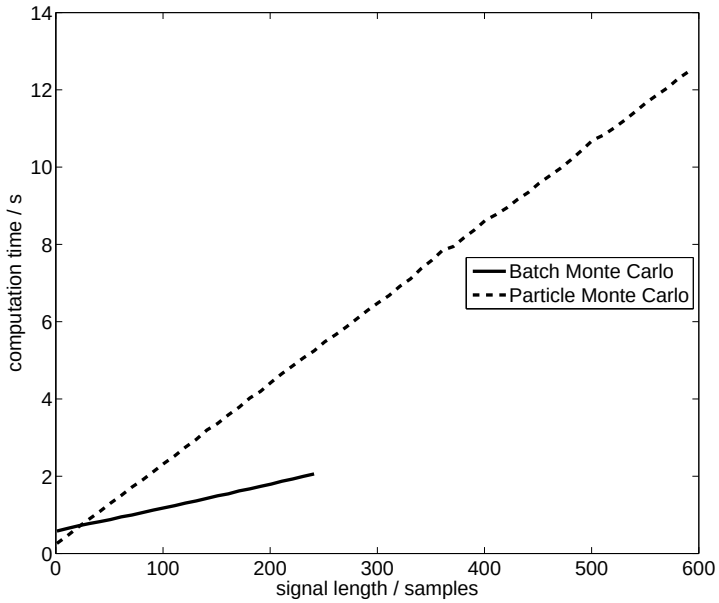

Figure 3.2: Computation time for PDF calculus for digital filtering by means of Particle Monte Carlo simulation (dashed) and Batch Monte Carlo simulation (solid) each with 10^5 number of sample draws. For signal lengths larger than 260 time samples, the Batch Monte Carlo method could not be performed on a standard PC with 32-bit operating system running MATLAB.

3.5 Regularisation

Deconvolution is an ill-posed problem [32]. An important property of ill-posed estimation problems is that the variance can be drastically reduced if the estimator is allowed to be biased [78]. This is also known as regularisation. As a consequence, the applied deconvolution filter is only an approximation to the exact inverse of the measurement system. Thus, every deconvolution filter introduces a systematic deviation which has to be accounted for in the uncertainty budget, unless it is negligibly small.

Let $z[n] = (g_{deconv} * y)[n]$ denote the result of a digital deconvolution filter applied to the (ideal) output signal $y[n] = y(nT_s)$ of the LTI system and define the corresponding systematic deviation $\Delta[n]$ as

$$\Delta[n] = z[n + n_d] - x[n],$$

where n_d denotes a possible time sample delay. Here we consider the ideal (noise-free) output signal $y(nT_s)$ to characterise the systematic deviation.

That is, owing to the application of the deconvolution filter, a systematic deviation remains even when an ideal noise reduction is realised.

In the following, we utilise the relation

$$X(e^{j\omega}) = \frac{1}{T_s} \sum_{k \in \mathbb{Z}} X(j(\omega + 2\pi k)/T_s)$$

between the Fourier transforms of $x(t)$ and its sampled version $x[n]$ together with an analogue relation for y; cf. [79].

We assume that knowledge about the LTI system's transfer function is characterised in terms of a parameter vector $\mathbf{\Gamma}$ and the deconvolution filter is obtained according to some mapping $f : \mathbf{\Gamma} \mapsto \mathbf{M}$ where $\mathbf{M}$ denotes the parameter vector of the deconvolution filter.

The goal is to take into account some prior knowledge about the measurand $x(t)$ to derive an upper bound for the systematic deviation $\Delta[n]$.

3.5.1 A particular type of prior knowledge

A reliable choice of regularisation parameters and a quantitative assessment of regularisation errors require taking some prior knowledge or assumptions about the estimated quantity into account. Here we consider a particular type of prior knowledge in the frequency domain, which we believe can be applied in many practical situations; cf. [80, 81].

Proposition 3.4. *Assume that knowledge about the measurand is given by means of an upper bound on the absolute value of its continuous Fourier transform*

$$|X(j\Omega)| \leq B(\Omega). \tag{3.23}$$

Then there exists an upper bound $\overline{\Delta} = \overline{\Delta}(B)$*, such that*

$$|\Delta[n]| \leq \overline{\Delta}$$

is independent of n*.*

Proof. The absolute value of the systematic deviation $\Delta[n]$ can be calculated

in the Fourier domain as

$$\begin{aligned}
|\Delta[n]| =& |z[n+n_d] - x[n]| \\
=& \frac{1}{2\pi} \Big| \int_{-\pi}^{\pi} e^{j\omega n} f_s \sum_k X(j(\omega f_s + 2\pi k f_s)) \\
& \times \left(e^{j\omega n_d} G_{\mu(\theta)}(e^{j\omega}) H_\theta(j(\omega f_s + 2\pi k f_s)) - 1 \right) d\omega \Big|. \qquad (3.24)
\end{aligned}$$

Inserting the assumed upper bound $B(\Omega)$ results in

$$\begin{aligned}
|\Delta[n]| \leq& \frac{1}{2\pi} \int_{-\pi}^{\pi} f_s \sum_k B(\omega f_s + 2\pi k f_s) \\
& \times \left| e^{j\omega n_d} G_\mu(e^{j\omega}) H(j(\omega f_s + 2\pi k f_s)) - 1 \right| d\omega \\
=& \frac{1}{2\pi} \int_{-\pi f_s}^{\pi f_s} \sum_k B(\Omega + 2\pi k f_s) \\
& \times \left| e^{j\Omega n_d / f_s} G_\mu(e^{j\Omega/f_s}) H(j(\Omega + 2\pi k f_s)) - 1 \right| d\Omega \qquad (3.25) \\
=:& \overline{\Delta}, \qquad (3.26)
\end{aligned}$$

where $\Omega = \omega f_s$ and $f_s = 1/T_s$. □

The value of (3.25) is determined by the compensation quality of the deconvolution filter G_μ and the presence of aliasing [13, 80]. More precisely, it is exactly zero for all input signals if

$$e^{j\Omega n_d / f_s} G_\mu(e^{j\Omega/f_s}) = \sum_{k \in \mathbb{Z}} H^{-1}(j\Omega + 2j\pi k f_s), \qquad (3.27)$$

which is satisfied when the deconvolution filter corresponds to the ideal filter and when no aliasing effects are present. For the latter, the sum on the right-hand side of (3.27) contains only one summand, namely that for $k = 0$.

Remark 3.3. *Strictly speaking, the upper bound $\overline{\Delta}$ defined in (3.26) remains unknown because the deconvolution filter G_μ is uncertain owing to the uncertainty associated with the LTI system's frequency response $H_\gamma(j\omega)$. However, since the deconvolution filter is constructed in dependence on the parameter vector γ, it can usually be assumed that $G_{f(\gamma)}(e^{j\Omega/f_s}) H_\theta(j\Omega + 2\pi j k f_s) \approx G_{f(\hat{\gamma})}(e^{j\Omega/f_s}) H_{\hat{\gamma}}(j\Omega + 2\pi j k f_s)$ holds. That is, the systematic deviation for the deconvolution filter designed w.r.t. to the estimate $\hat{\gamma}$ and some filter that has been designed w.r.t. to the underlying γ can be expected to be essentially the same.*

Knowledge about the dynamic error is then given by means of $\Delta[n] \in [-\overline{\Delta}, \overline{\Delta}]$ for all n. We model the state of knowledge about the value of $\Delta[n]$ using the uniform PDF

$$p_{\Delta[n]}(\delta) = \begin{cases} \frac{\overline{\Delta}}{2} & |\delta| \leq \overline{\Delta} \\ 0 & \text{otherwise} \end{cases} . \tag{3.28}$$

The uncertainty contribution of the systematic deviation is then given by the variance of this PDF and the resulting squared uncertainty associated with $\hat{x}[n]$ is given by

$$u^2(\hat{x}[n]) = u^2((g_\mu * y)[n]) + \frac{\overline{\Delta}^2}{3}. \tag{3.29}$$

Hence, when the uncertainty contribution of the regularisation error is accounted for, the resulting uncertainty consists of a signal variance term and a bias term. The regularisation scheme considered here is a cascade of a compensation filter and a low pass filter. Assuming that the contribution of the compensation filter to the upper bound on the time domain deviation is negligible or fixed, the low pass filter can be employed to control both terms of equation (3.29). A narrow pass band of the low pass filter results in a strong reduction of signal noise, but increases the bound on the deviation $\overline{\Delta}$. Thus, the low pass filter cut-off frequency allows a determination of the trade-off between the noise reduction and bias reduction. In the following, we employ this concept for the design of an (approximately) uncertainty-optimal deconvolution filter.

3.5.2 Uncertainty-optimal filtering

The assumed knowledge of an upper bound $B(\Omega)$ for the calculation of an upper bound of the systematic deviation $\Delta[n]$ allows for a quantitative assessment of the quality of the employed deconvolution filter. Hence, it can be used to determine a deconvolution filter, which results in minimal uncertainties.

Similar to the classic approaches for regularised deconvolution (1.13) and (1.14), we consider the deconvolution as a cascade of a compensation filter and a low pass filter

$$g(z) = g_{low}(z) g_{comp}(z).$$

The compensation filter is designed such that it approximates the inverse of the measurement system model within a certain frequency range. The low pass filter is employed to attenuate noise. Thereby, the low pass filter reduces the variance of the input signal estimate, but also introduces a bias. This effect can be controlled by the low pass filter cut-off frequency [13]. Design of an (approximately) uncertainty-optimal deconvolution filter can thus be carried out by Algorithm 3.

Algorithm 3: Desing of uncertainty-optimal filter

1 1. Design the compensation filter g_{comp} such that;

2

$$G_{comp}(e^{j\Omega T_s}) \approx H^{-1}(j\Omega)$$

for $\Omega \in [0, \Omega_{up}]$;

3 2. Determine the low pass filter cut-off frequency such that

$$\text{mean}_{n=0,\ldots,N}\, u^2(\hat{x}[n]) \tag{3.30}$$

is minimised.

The optimisation criterion (3.30) can be adapted to account for specific situations. For instance, in some cases the maximum value over a certain interval or a weighted mean may be preferable.

The bound on the systematic dynamic error $\Delta[n]$ allows for a trade-off between variance reduction and bias reduction. This is illustrated in Fig. 3.3 for a simulated example. For small values of the low pass filter cut-off frequency, the systematic deviation is large, whereas the variance of the estimate increases for large cut-off values. Accounting for both contributions according to Eq. (3.29) then results in the parabola-like function shown for the maximum value of uncertainty. The minimal value of the parabola then corresponds to the optimal trade-off between variance and bias in terms of minimal uncertainty. The resulting deconvolution filter is thus (approximately) uncertainty-optimal.

The employed concept of regularised deconvolution is related to the classic approaches discussed in Section 1.2.3. However, contrary to the Tikhonov deconvolution filter (1.14), the low pass filter is not determined by some penalty operator. Moreover, the cut-off frequency is not chosen heuristically, e.g., by the L-curve method as applied in [29]. For a suitably chosen type of low pass filter, the deconvolution filter obtained by the proposed procedure can be expected to be comparable to the Wiener filter. Therefore, take $B(\Omega)$

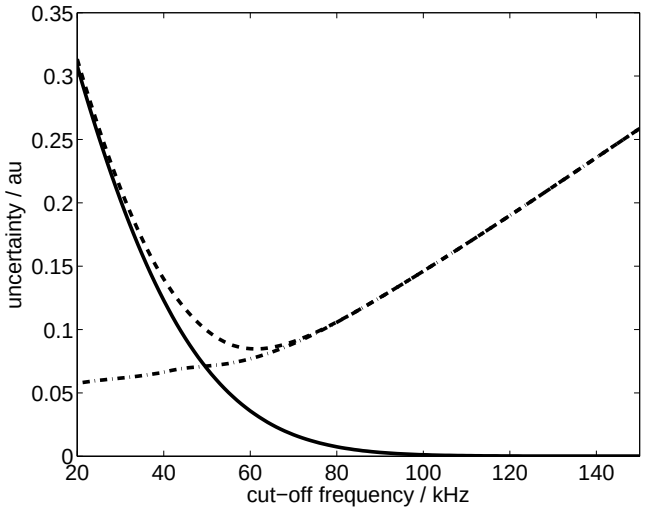

Figure 3.3: Maximal value of the uncertainty without accounting for the systematic deviation (dash-dotted), without accounting for signal noise and system uncertainty (solid) and the overall uncertainty (dashed).

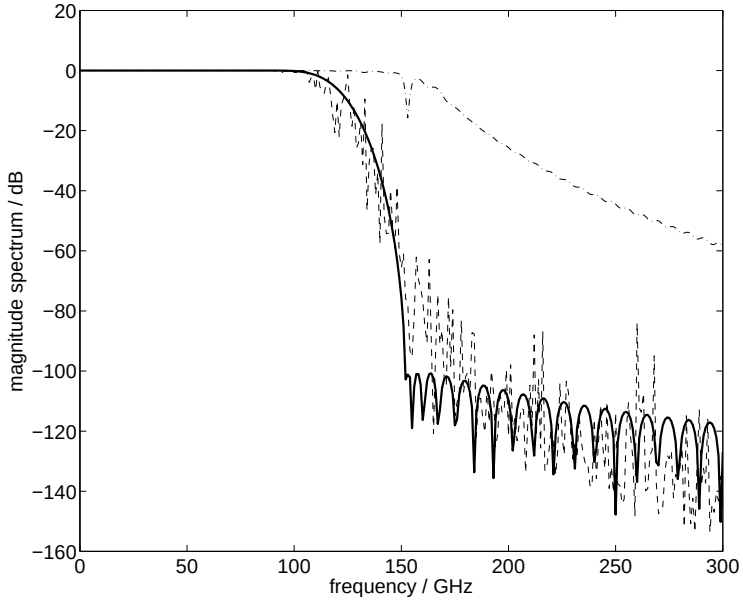

Figure 3.4: Frequency response of a compensated system for the application of Wiener deconvolution (dashed), Tikhonov deconvolution with second-order difference operator (dash-dotted) and the inverse system followed by a FIR low pass filter (solid).

as the power spectrum of a wide-sense stationary process. Then, the equation (1.13) for the calculation of the Wiener filter results in the deconvolution filter frequency response

$$G_W(j\Omega) = H^{-1}(j\Omega)\frac{|H(j\Omega)|^2}{|H(j\Omega)|^2 + N(j\Omega)/B(\Omega)},$$

with $N(j\Omega)$ representing the power spectrum of the observation noise process. Figure 3.4 shows the compensation result obtained as the cascade of the system frequency response and the compensation filter for the Tikhonov deconvolution, the Wiener filter w.r.t. the assumed bound and the design method proposed here. The example corresponds to the oscilloscope example in Section 4.4. Determination of the Tikhonov regularisation parameter λ has been carried out by the L-curve method as in [29]. Figure 3.4 shows that the deconvolution filter obtained by Algorithm 3 has a similar transfer function as the Wiener filter, which is usually considered as the optimal deconvolution filter in classical DSP applications. However, an optimisation criterion based on measurement uncertainty is more suitable for applications in metrology than the root-mean-square error criterion for the Wiener filter. Moreover, the measurand in metrological applications is usually not a stochastic process.

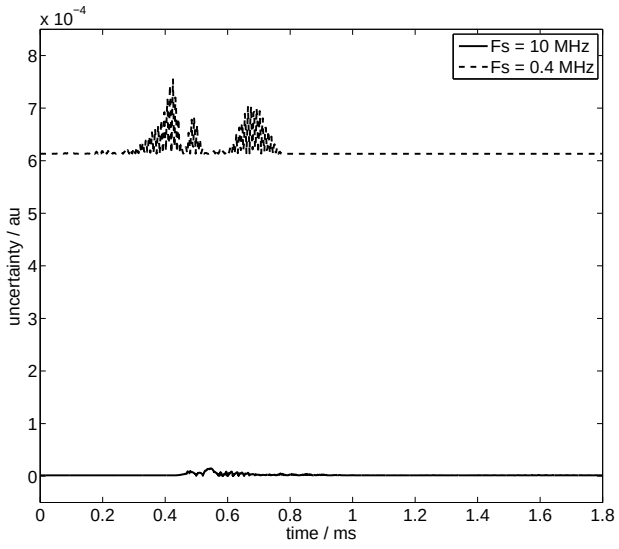

Figure 3.5: Uncertainties associated with an estimate obtained from an observation sampled with 10 MHz (solid) and 0.4 MHz (dashed), respectively.

Since the assumed bound function $B(\Omega)$ is continuous, it also allows for an assessment of uncertainty contribution due to aliasing effects. This is illustrated in Fig. 3.5 for an example related to Section 4.5. The observed output signal is sampled with two different sampling frequencies and the deconvolution filter designed by Algorithm 3 with the parameters as given in Section 4.5.

Chapter 4

Applications

4.1 Outline

Dynamic measurements are a topic of growing importance in metrology and the methodologies proposed here can be applied for a wide range of dynamic measurements.The measurement of dynamic acceleration is currently the best investigated quantity and parts of the methods presented in this section are already applied in practice. In Section 4.5, we extend the currently available methodologies for uncertainty-optimal filtering and continuous-time estimation developed here. This allows the complete measurement analysis in Fig. 2 to be considered for the first time. In particular, the relation of the discrete-time estimate $\hat{x[n]}$ to the continuous-time measurand $x(t)$ can now be derived.

Dynamic calibration of sampling oscilloscopes is currently performed at a small number of national metrology institutes (NMIs). Up to now the research in this area has focused on non-parametric characterisation. In Section 4.4, we demonstrate that the methodology for uncertainty-optimal filtering developed here can also be applied for the corresponding non-parametric estimation methods. The applied regularisation then results in more reliable uncertainties than for the often heuristic regularisation methods used in this area.

Dynamic calibration of transducers and sensors for the quantities force, torque and pressure has only recently been considered. The first results for force

calibration can be found in [12]. Some results for dynamic calibration of a pressure sensor are given in Section 4.2. The traceable dynamic calibration of torque transducers is still at a preliminary stage. In fact, the EMRP-IND09 project started in September 2011 will establish traceable primary calibration for these quantities for the first time.

The range of applications in metrology which already require analysis of dynamic measurements, demonstrates the need for a harmonised treatment for the evaluation of dynamic measurement uncertainty. Hence, the framework for the analysis of dynamic measurements presented here is of great benefit for a wide range of applications. In the following, we present more details for the individual quantities to illustrate the benefits of the proposed framework.

4.2 Pressure

Measurement of dynamic pressure is necessary, for instance, in ballistics or in-engine car measurements. The required dynamic range (amplitude and frequency) in such applications is typically very high. Calibration of pressure transducers for their application under highly dynamic conditions can be performed by employing shock tube measurements [82, 83]. Development of a corresponding primary standard will be carried out as part of the EMRP IND09 project "Traceable dynamic measurement of mechanical quantities" that began in 2011.

Presently, one difficulty in the use of a shock tube as a primary standard is the lack of knowledge about the pressure value at the end wall of the tube where the sensor is located. Based on FEM simulations, we focused on a step function model as the assumed input signal in these calibrations. This allowed us to infer a frequency response function of the pressure sensor from its observed outputs assuming that the assumed input signal corresponds to the true input signal. In Fig. 4.1 the resulting frequency response is shown for one data set of a shock tube measurement at the National Physics Laboratory (NPL) in the UK (see also [84]). From the manufacturer's data sheets for the employed measurement devices, a parametric model for the measurement system was derived as a damped mass-spring system followed by a 6th order Butterworth analogue low pass filter. A first calibration of the pressure sensor was then carried out by a least squares approach and an estimation of uncertainties. The frequency response of the obtained parametric model is also shown in Fig. 4.1. Although the assumed model shows reasonable char-

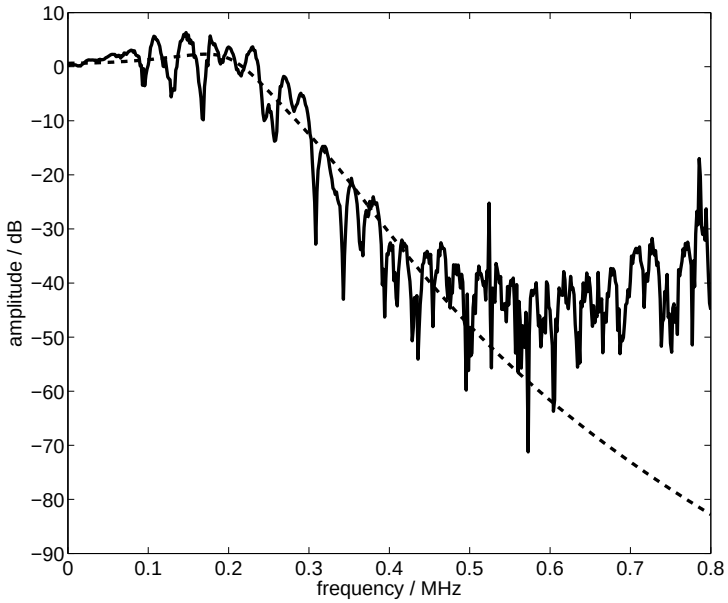

Figure 4.1: Amplitude of the inferred frequency response function (solid) of the measurement system in calibration measurements with a shock tube. Also shown is the frequency response of an identified parametric model for the transducer (dashed).

acteristics for the identified model parameters, the model response shows significant deviations from the inferred non-parametric frequency response. Accounting for these deviations and investigating more advanced input pressure signal models will be part of the research in EMRP IND09. Application and validation of the calibration results requires an analysis of dynamic measurements for which the framework presented here can be applied.

4.3 Force

Measurement of dynamic force occurs, for instance, in automobile crash tests or fatigue testing machines. Calibration of force transducers under dynamic conditions has recently been considered, such as in [12]. The authors identified a parametric mathematical model for the force transducer from calibration experiments with sinusoidal excitations. However, the assumed model and the identified parameters are very sensitive to the conditions of the calibration experiments. Moreover, validation of the results by means of compar-

isons with measurements performed by other laboratories has not yet been carried out due to a lack of such facilities. Research and development in this direction is part of the EMRP IND09 project. As a result of this project, the methodologies proposed here can then be applied to analyse measurements of dynamic force.

4.4 Sampling oscilloscopes

4.4.1 Dynamic calibration

Ultra-fast sampling oscilloscopes with nominal bandwidth of over 70 GHz are employed for high-speed instrumentation measurements. Dynamic calibration of sampling oscilloscopes has been considered, for instance, in [28, 31, 85]. The calibration result is a discrete-time estimate of the impulse response together with an associated uncertainty. In [31], uncertainty calculus has been considered, whereas we applied PDF calculus in [85]. So far, no parametric model has been identified for these systems. Hence, the discrete-time values of the impulse response are considered as parameters.

In order to demonstrate the applicability of the proposed framework we employ a calibrated impulse response of a sampling oscilloscope with nominal bandwidth of about 100 GHz and use a *simulated* input signal to calculate a simulated output. The chosen input signal is closely related to the measurements presented in [29]. Likewise, we assign an uncertainty to our simulated output signal which shows similar characteristics as those in [29].

4.4.2 Simulated input signal

Application of the calibration result for the calibration of pulse generating devices has been considered in [29]. Here, we illustrate the analysis of such pulse measurements by means of a simulated example. That is, we apply the actual calibrated impulse response shown in Fig. 4.2 to a simulated input signal to calculate a simulated response of the sampling oscilloscope. For estimation of the input signal, we adopt the methodologies proposed here to a deconvolution in the frequency domain. Moreover, we consider the input signal to be discrete-time. Consequently, the bound function B for the

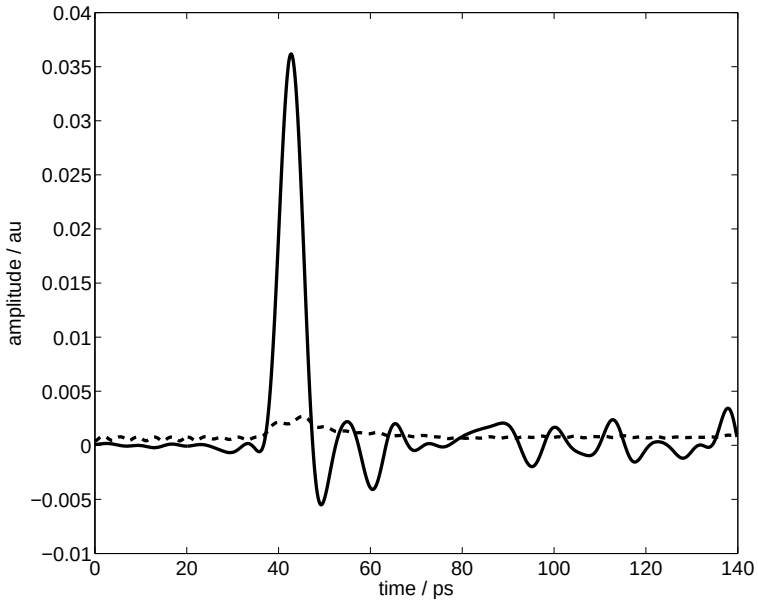

Figure 4.2: Calibrated impulse response for a sampling oscilloscope with nominal bandwidth of about 100 GHz (solid) and the associated uncertainties (dashed).

proposed regularisation scheme is derived from a DFT transform.

More precisely, as input signal, we consider a pulse of unit height approximated by a scaled and shifted Gaussian error function $erf((t-\tau_p)/\sigma_p)$ with $\sigma_p = 5$ and $\tau_p = 200$ ps. As a measurement system, we considered a dynamically calibrated sampling oscilloscope with calibrated impulse response shown in Fig. 4.2. The simulated output signal is shown in Fig. 4.3 together with the associated uncertainties. Calculations are performed in the Fourier domain employing the ramp subtraction approach proposed in [29].

We assigned uncertainties to the simulated output, which shows similar characteristics as those of the actual pulse measurements in [29]. Therefore, the value of the uncertainties has been assigned as $u^2(s[n]) = \mathrm{grad}(s[n])^2 + \sigma_{noise}^2$ with $\sigma_{noise} = 0.001$ and grad denoting the central differences operator applied to the simulated output signal.

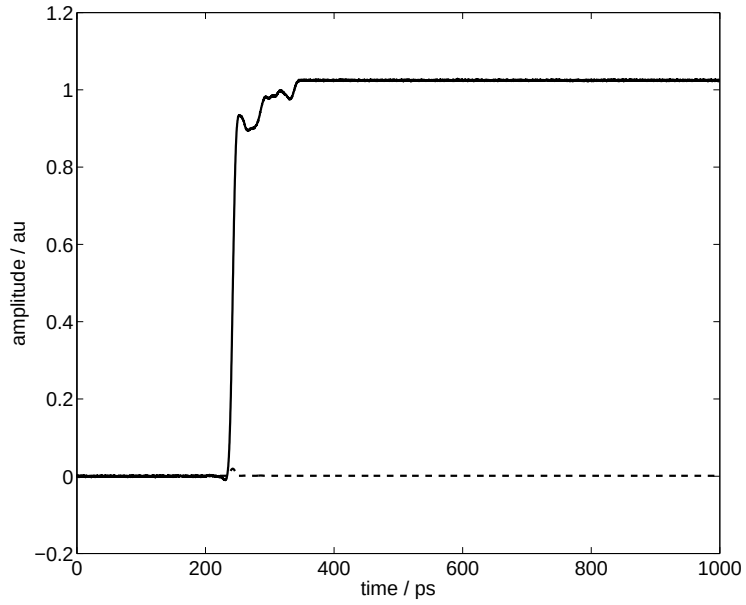

Figure 4.3: Simulated response of oscilloscope to step-like input signal (solid) and associated uncertainties (solid).

4.4.3 Uncertainty-optimal deconvolution

We carry out deconvolution in the discrete frequency domain similarly to how it is done in [29]. A Tikhonov approach has been applied in [29], resulting in a discrete variant of Eq. (1.14). Therefore, the regularisation parameter was determined by the so-called L-curve method based on a local quadratic approximation.

Here we apply the proposed methodology of a bound in the Fourier domain, for which we apply the DFT of a rectangular-like signal with similar side-wall slope as the simulated input pulse (see Section 3.5). Since we consider simulations, knowledge about the actual frequency content of the input signal is available. In an application, the slope of the assumed rectangular-like signal can be chosen based on some prior knowledge about the considered pulse generator.

The deconvolution sought is a cascade of the reciprocal system and a low pass filter $H_d(\omega) = H^{-1}(\omega)H_{lp}(\omega)$ (see Section 3.5). As a low pass filter, we apply an order 500 FIR filter designed by the window technique with a Kaiser window [13]. The window scale parameter is chosen as 10. Design of an

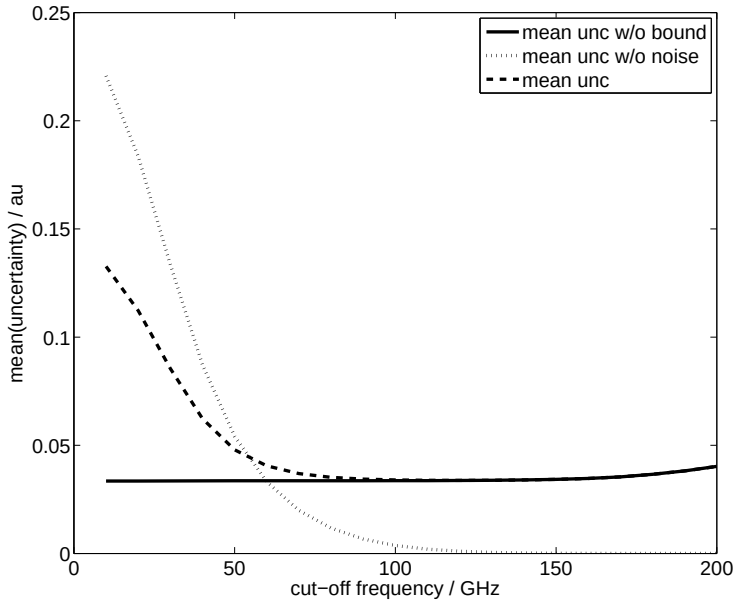

Figure 4.4: Mean value of uncertainty without accounting for systematic deviation (solid), without accounting for noise and system uncertainty (dotted) and mean uncertainty (dashed). The optimal cut-off frequency for this example is found to be 116 GHz.

uncertainty-optimal deconvolution filter is then carried out by determining an optimal low pass cut-off frequency for the low pass filter (see Section 3.5.2).

We employed Monte Carlo simulations to implement PDF calculus (see Section 1.1). Figure 4.4 illustrates the impact of the low pass filter cut-off frequency on the different contributions to the uncertainty. In Figure 4.5, the estimate of the measurand for the optimal cut-off frequency of 116 GHz is shown together with the associated uncertainties.

Contrary to the methodology in [29], our approach allows for an uncertainty-optimal deconvolution by accounting for the uncertainty contribution of the regularisation error.

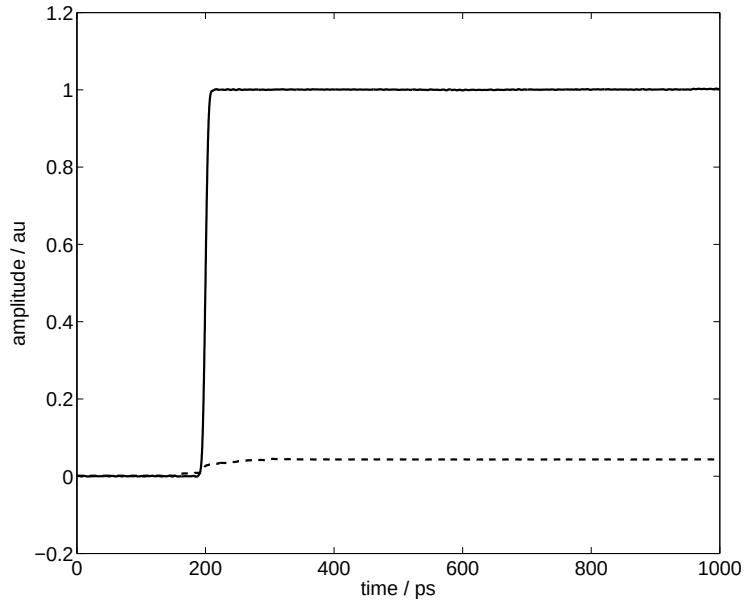

Figure 4.5: Estimate of input signal (solid) together with the associated uncertainties (dashed).

4.5 Acceleration

Dynamic calibration of accelerometers has been considered in [9, 26]. The authors showed that a dynamic treatment of shock calibration experiments is necessary for the comparison of different shock measurements.

We extend these results by illustrating the methodologies proposed here for the analysis of a dynamic measurement with a dynamically calibrated accelerometer. We consider measurements performed with a sensor manufactured by the company Endevco®. The considered sensor is of the type 2270 with serial number BA67. Calibration of the sensor has been carried out for sinusoidal calibration measurements (see [26]).

The measurements considered here are shock excitations with peak values of about 80 km/s^2. Figure 4.6 shows the corresponding sensor output signal. For the measurements, an estimate of the actual input signal is available from interferometer measurements.

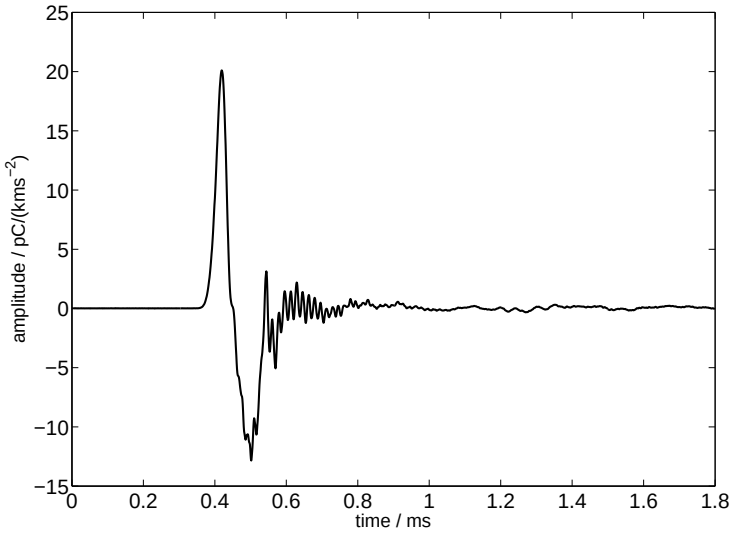

Figure 4.6: Sensor output signal for a shock excitation with a peak value of about 80 km/s^2.

4.5.1 Design of compensation filter

The calibrated continuous-time parametric model of the sensor allows for the calculation of the frequency response at arbitrary frequency values and their associated uncertainties. We consider a discrete set of frequency response values in the frequency range from 0 Hz to 100 kHz. To these values we determine a weighted linear least squares solution for the equation

$$H^{-1}(j2\pi f) = G_\mu(e^{j2\pi f F_s}) \qquad f_1 \ldots, f_M \in [0, 10^5]$$

to determine the filter parameters $\boldsymbol{\mu}$ of an FIR type digital filter; cf. [40]. The filter order of the compensation filter is chosen as 30 with a time sample delay of $n_d = 15$ samples. Evaluation of uncertainty for the compensation filter coefficients is carried out as a propagation from the uncertainty associated with the frequency response values through the linear least squares estimation.

4.5.2 Regularisation

For regularisation, we employ a low pass filter in cascade to the FIR compensation filter. In order to quantify the uncertainty contribution of the low pass filter we use a continuous function $B(\Omega)$ as an assumed upper bound to the amplitude of the Fourier transform of the continuous time sensor input signal; cf. Section 3.5. In order to derive a model for the continuous bound function the shock excitation signal is roughly modeled as two subsequent Gaussian pulses with equal height, but opposite sign as

$$x_{model}(t) = h\exp(-\frac{1}{2\sigma^2}(t-t_1)^2) - h\exp(-\frac{1}{2\sigma^2}(t-t_2)^2).$$

The height parameter h corresponds to the employed peak excitation. The parameter σ determines the bandwidth of the upper bound $B(\Omega)$ as

$$\sigma = \sqrt{\log 2}/(2\pi \cdot \text{bandwidth}).$$

Generally, choosing a model and its parameters for $B(\Omega)$ requires some prior knowledge or assumptions. Here we assume that prior knowledge leads to an assumed bandwidth = 9 kHz for the considered peak excitations of about 80 km/s^2. For the time instants t_1, t_2, we assume that no prior knowledge about its values is available.

The Fourier transform of the assumed model $x_{model}(t)$ is given by

$$X_{model}(\Omega) = h\sqrt{2\pi\sigma^2}\exp(-\frac{1}{2}(\Omega)^2)(\exp(-j\Omega t_1) - \exp(-j\Omega t_2)).$$

To determine the upper bound function $B(\Omega)$, we bound $|X_{model}(\Omega)|$ from above as

$$\begin{aligned} |X_{model}(\Omega)| =& h\sqrt{2\pi\sigma^2}\exp(-\frac{1}{2}(\Omega)^2)|\exp(-j\Omega t_1) - \exp(-j\Omega t_2)| && (4.1)\\ \leq& h\sqrt{2\pi\sigma^2}\exp(-\frac{1}{2}(\Omega)^2) \times 2, && (4.2)\end{aligned}$$

where the factor 2 results from bounding $|X_{model}(f)|$ from above, taking into account that t_1 and t_2 are assumed to be unknown. Hence, we define the upper bound on the magnitude spectrum of $x(t)$ as

$$B(\Omega) = 2h\sqrt{2\pi\sigma^2}\exp(-\frac{1}{2}(2\pi f)^2). \quad (4.3)$$

In Fig. 4.7, the resulting function $B(\Omega)$ is shown together with a discrete Fourier transform of the measured input.

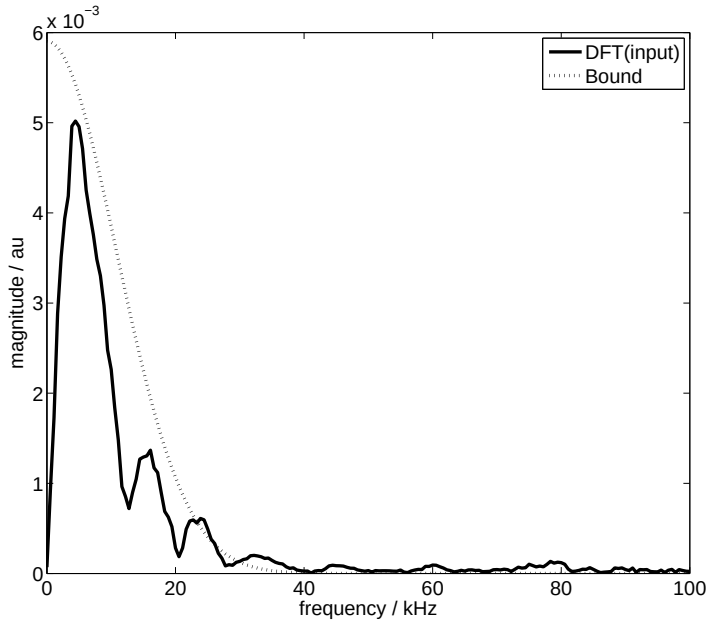

Figure 4.7: Magnitude of DFT of sensor input signal (solid) and assumed continuous bound function $B(\Omega)$ (dashed).

4.5.3 Optimisation of low pass filter

As a low pass filter, we apply an FIR filter of order 600 designed by the window technique with a Kaiser window scaling factor equal to 16. The filter order and window scaling factor have been determined by the MATLAB routine *kaiserord* with design parameters $Fpass = F_c - 5$ kHz, $Fstop = F_c + 5$ kHz with F_c the filter cut-off frequency being sought. The sought bound on the pass band ripples has been chosen as 10^{-4} and the stop band ripples as -40 dB.

The resulting additional time sample delay of 300 samples appears to be rather high. However, the reason for the large low pass filter order is that the ratio of cut-off frequency sought and the sampling frequency is in the order of 0.1%. An IIR low pass filter would significantly reduce the required filter order with the trade-off of a non-linear phase response. However, the approximate time sample delay for the IIR filters would also be of the order of about 100 samples. See [86] for the case of a Butterworth filter.

The assumed upper bound (4.3) can be employed to determine an optimal cut-off frequency for the additional low pass filter (see Section 3.5.2). To

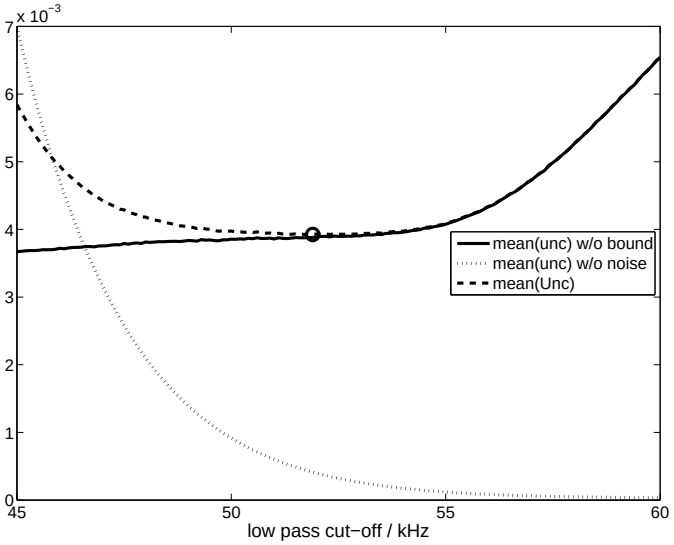

Figure 4.8: Mean value of uncertainty for the estimated sensor input signals for the BA67 sensor when the bound is not taken into account (solid), the uncertainty when the bound is taken into account (dotted) and the value of the bound (dashed) viewed as the uncertainty without accounting for noise. Also shown is the estimated optimal value for the cut-off frequency, which is 51.9 kHz.

this end, we perform a grid search from 45 kHz to 60 kHz with a grid size of 0.1 kHz to find an approximate minimum of

$$F(\omega_c) = \text{mean}_{n=1,\ldots,M} \left\{ u^2((g_{comp} * (g_{low} * y))[n]) \right\},$$

which depends on the output signal noise variance, the uncertainty associated with the compensation filter and the bound on the systematic deviation as a function of the low pass filter cut-off frequency (see Algorithm 3 in Section 3.5).

In Fig. 4.8, the expected trade-off between small bias and small variation due to noise can be seen; cf. Section 3.5.2. Note that for larger noise variance in the output signal, the increase of the maximal uncertainty values for larger cut-off frequencies would be significantly larger.

Figure 4.9 shows the resulting frequency response of the deconvolution filter. Also shown is the product of the sensor model frequency response and that of the deconvolution filter to illustrate the compensation quality of the applied filter.

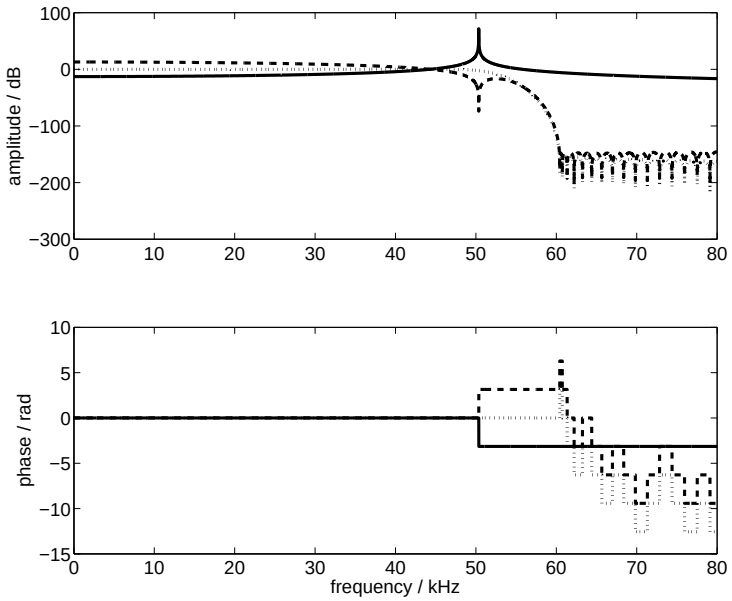

Figure 4.9: Top: Magnitude spectrum of sensor model frequency response (solid), digital deconvolution filter frequency response (dashed) and that of the resulting compensated system (dotted). Bottom: Corresponding phase spectra.

4.5.4 Input estimation

The deconvolution filter designed is applied to the measured output signal of the accelerometer illustrated in Fig. 4.6. Hence, the estimate of the input signal is calculated as

$$\hat{x}[n] = (g_{comp} * (g_{low} * y)[n + n_d],$$

where y denotes the sensor output signal and g_{low}, g_{comp} denotes the low pass filter and compensation filter, respectively.

4.5.5 Evaluation of uncertainty

We estimate the noise variance from the first 0.3 ms of the output signal, where no significant signal amplitude is present. The estimated noise standard deviation is $\sigma_n = 3.1e - 3$. The uncertainty of the compensation filter has been determined by uncertainty propagation from the identified sensor model to the compensation filter coefficients.

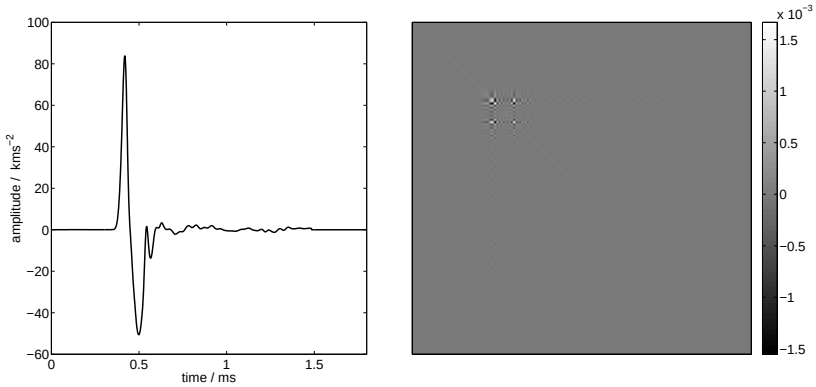

Figure 4.10: Left: Estimate of sensor input signal. Right: Covariance matrix encoding the mutual uncertainties.

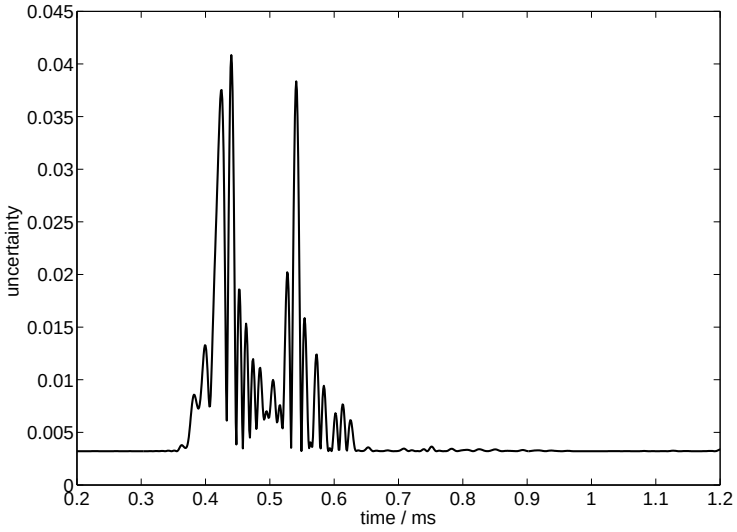

Figure 4.11: Dynamic uncertainty as the square root of the diagonal entries of the covariance matrix.

The estimation result for one measurement with the above shock intensities for the BA67 sensor is shown in Fig. 4.10 together with the obtained matrix of mutual uncertainties $u(\hat{x}[n], \hat{x}[m])$. The uncertainties at the individual time instances are shown in Fig. 4.11.

4.5.6 Continuous-time estimate

From the discrete-time estimate $\hat{x}[n]$, $n = 0, \ldots, N$ a continuous-time estimate can be obtained as proposed in Section 2.4.

Uncertainty is assigned to this estimate by means of the associated continuous-time stochastic process

$$X_t = \sum_{n=0}^{N} x[n] sinc\left(\frac{t - nT_s}{T_s}\right),$$

which models the state of knowledge about the continuous-time input signal $x(t)$. From the stochastic process, a "credible region" in the space of continuous functions can be estimated by application of Proposition 2.1. Therefore, we applied this proposition with g equal to the mean function $m_X(t)$, and determined an upper bound β such that the probability of $M(\omega)$ is about 95%. The resulting 95% "credible region" is shown in Fig. 4.12. This region can be interpreted to contain the degree of belief that the true continuous function is located in this region with 95% probability. In Fig. 4.12, it can be seen that this region is very small in the considered example, which is due to a relative uncertainty associated with the discrete-time estimate of about 0.5%.

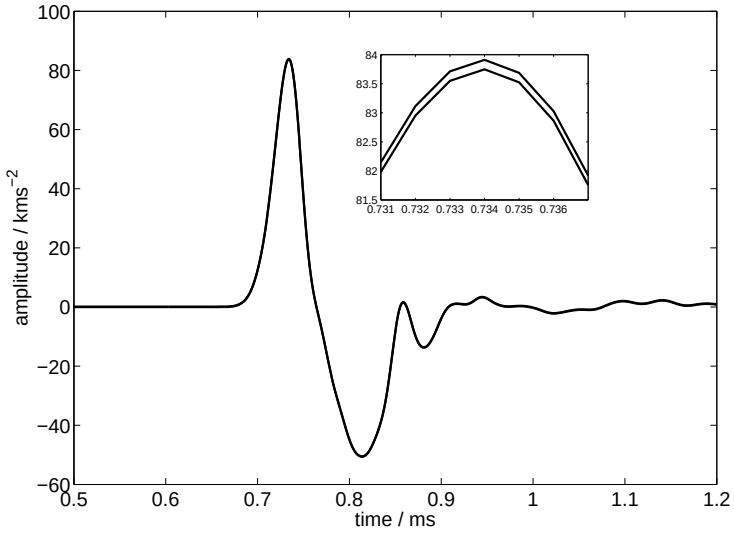

Figure 4.12: Approximated credible region in the function space for the estimated continuous-time sensor input signal with approximately 95% probability obtained from the assigned stochastic process. Owing to the small uncertainties, the credible region on this scale appears as one line. The small inset figure shows the segment around the signal maximum.

Chapter 5

Conclusions and outlook

The analysis of dynamic measurements is a topic of growing importance in metrology and industry. In an increasing number of applications, the dynamic behaviour of the measurement device applied has to be taken into account in order to obtain good estimates and reliable associated uncertainties. The calibration and measurement of static quantities is well-established. For the corresponding evaluation of static measurement uncertainty, the GUM and its supplements provide a framework in metrology. However, extending these guidelines to the treatment of dynamic measurements has only recently been considered.

In this thesis, we focused on measurement systems that can be modelled by a linear and time invariant (LTI) system since such models cover a wide range of metrological applications. The goal in the analysis of a dynamic measurement is the estimation of the dynamic measurand which serves as input signal to the measurement device; cf. Fig. 2 in the Introduction. This requires (i) a calibration of the measurement device characterising its dynamic behaviour, (ii) a method for calculating a (discrete-time) estimate of the (continuous-time) measurand from the observed (discrete-time) measurement device response signal and (iii) a methodology to relate the discrete-time estimate to the continuous-time measurand. For each of the aspects (i) to (iii), an evaluation of measurement uncertainty in accordance with the established guidelines in metrology is required in order to enable traceability of the measurement result to national and international standards.

Dynamic calibration (i) is a recent topic of research in metrology, such as the European Metrology Research Project IND09 started in September 2011.

In this thesis, we focused on aspects (ii) and (iii). Therefore, we assumed that a dynamic calibration has been carried out and provides a dynamic characterisation of the measurement device with an associated uncertainty. Discrete-time estimation (ii) via deconvolution is well-established in the digital signal processing (DSP) literature. Typically, based on the knowledge about the measurement device, a digital filter is designed, whose input is the observed sensor output signal and whose output is a discrete-time estimate of the corresponding sensor input signal. Also well-established in the DSP literature is the propagation of (noise) variances through digital filters. However, this is only one contribution to the measurement uncertainty associated with the input signal estimate. Other important uncertainty contributions arise from the estimation filter. Due to imperfect knowledge about the measurement device, the deconvolution filter's parameters are uncertain. Moreover, deconvolution requires regularisation, which in turn results in systematic estimation errors. The propagation of uncertainty associated with the dynamically calibrated device to an uncertainty associated with the parameters of the digital deconvolution filter can be carried out as described in the GUM and its related documents. Closed formulas have been recently developed for the propagation of standard uncertainties to the result of the deconvolution, i.e., the input signal estimate.

The main results of this thesis are as follows: We developed a concept to calculate the uncertainty contribution of the regularisation error in the deconvolution. This extends previous approaches, which do not account for the regularisation error. The formulas developed here provide a complete uncertainty evaluation for the application of digital deconvolution filters. We employed this approach to outline a procedure for designing a deconvolution filter with respect to the resulting measurement uncertainty associated with the input signal estimate. The proposed approach results in smaller and more reliable uncertainties. Moreover, the previous approaches focused on the mean and covariances and, for IIR filters, required a linearisation of the measurement equation. We extended these approaches by an application of the propagation of PDFs by a Monte Carlo method as described in GUM supplements 1 and 2. Due to the high-dimensional character of the estimation problem, the application of Monte Carlo methods for dynamic measurements is impractical on most computers. To this end, we developed an algorithm for an efficient implementation of the Monte Carlo method. It allows for an evaluation of uncertainties and (point-wise) credible intervals with a large

number of simulation runs even on standard desktop computers. Since the accuracy of the Monte Carlo result mainly depends on the number of Monte Carlo simulations, this efficient implementation is an important contribution to a reliable measurement result.

Typically, the sensor output signal is observed in discrete-time. Hence, the estimation algorithms are based on DSP methods. However, the measurand is actually a continuous-time function. The GUM does not consider continuous functions as a measurand. Therefore, we extended their methodologies to a general framework for continuous functions. This framework is based on stochastic processes to encode uncertain knowledge about the values of the function. It can be applied beyond dynamic measurement analysis, for instance, in the field of continuous modelling. The framework developed here addresses the assignment and propagation of the uncertainty associated with a continuous function through linear or linearised operators. It provides an uncertainty calculus for continuous functions, which is exact for linear operators and functionals. Finally, we related this new framework with the previously developed discrete-time estimation methods. Therefore, the discrete-time estimate and its associated uncertainty (or PDF) are employed to define a parametrised continuous-time stochastic process. This stochastic process encodes the state-of-knowledge about the continuous-time measurand. In this way, a continuous-time estimate with an associated uncertainty can be calculated from the discrete-time estimate.

For the first time, the methodologies developed here close the circle of the measurement analysis illustrated in Fig. 2 in the Introduction. That is, the methods developed in this thesis allow for a complete analysis of a dynamic measurement in line with the guidelines for uncertainty evaluation in metrology.

Outlook

In this thesis, we focused on measurement devices which can be modelled by linear and time invariant systems since such models cover a wide range of applications in metrology. However, in future research, the methodologies developed here could be extended to general non-linear models. This includes measurements that are modelled by partial differential equations. One approach may be to employ a first order Volterra series as a means of a linearisation of non-linear operators. This would be related to a GUM uncer-

tainty calculus approach that relies on a first order Taylor series expansion of non-linear functions. Another approach may be to consider non-linear operators and functions directly and to extend the calculus for continuous functions developed here to the treatment of non-linear operators. For the discrete-time deconvolution, we here focused on linear digital filters. Future research may consider non-linear filters to carry out the deconvolution. For instance, instead of a linear low-pass filter for regularisation, a non-linear filter may provide better noise attenuation properties.

Another direction for future research could be the optimisation of the measurement analysis. For instance, one may consider an optimal design of experiment for the dynamic calibration with respect to the uncertainty associated with the input signal estimate in the measurement stage. It would also be interesting to further investigate the concept developed here for the design of uncertainty-optimal deconvolution filters. We focused on a particular type of prior knowledge about the measurand and the optimisation of the low-pass filter cut-off frequency. This may be extended to different types of prior knowledge or a multi-parameter optimisation of low-pass filter characteristics.

Acknowledgments

Many thanks to my working group leader at PTB, Dr. Elster, and my colleague Dr. Link for their comments, suggestions and explanations and many thanks for their patience with me in countless discussions which all turned out to be very fruitful for this thesis. I also wish to thank my supervisor Prof. Bär for taking me on board and supporting me. Thanks also to my colleagues at PTB Braunschweig and at NPL (UK), who allowed me to use their measurements for my studies and many thanks to Franko, who helped me with the pre-processing of this data.

Proofreading of the final draft of this thesis by the company *proofreading.de* is gratefully acknowledged.

Lastly, and most important, I wish to thank my whole family for their support and encouragement. This would not have been possible without you.

Bibliography

[1] WTO. Technical barriers to trade. website. "Available online at `http://www.wto.org/english/tratop_e/tbt_e/tbt_e.htm`; visited on July 25th 2011".

[2] BIPM. World Metrology Day. website. Available online at `http://www.bipm.org/en/convention/wmd/`; visited on July 25th 2011.

[3] BIPM, IEC, IFCC, ISO, IUPAC, IUPAP, and OIML. *Guide to the Expression of Uncertainty in Measurement*. International Organization for Standardization, Geneva Switzerland, 1995.

[4] BIPM, IEC, IFCC, ISO, IUPAC, IUPAP, and OIML. *Evaluation of Measurement Data - Supplement 1 to the 'Guide to the Expression of Uncertainty in Measurement' - Propagation of Distributions Using a Monte Carlo Method*. Joint Commitee for Guides in Metrology, Bureau International des Poids et Mesures, JCGM 101, 2008.

[5] BIPM, IEC, IFCC, ISO, IUPAC, IUPAP, and OIML. *Evaluation of Measurement Data - Supplement 2 to the 'Guide to the Expression of Uncertainty in Measurement' - Extension to any number of output quantities*. Joint Commitee for Guides in Metrology, Bureau International des Poids et Mesures, JCGM 102, 2011.

[6] BIPM. JCGM working group on the expression of uncertainty in measurement. website. Available online at `http://www.bipm.org/en/committees/jc/jcgm/wg1.html`; visited on July 25th 2011.

[7] T. J. Esward, C. Elster, and J. P. Hessling. Analysis of dynamic measurements: new challenges require new solutions. In *XIX IMEKO World Congress on Fundamental and Applied Metrology*, 2009.

[8] EURAMET. EMRP Call 2010 - Industry and Environment. website. Available online at `http://www.euramet.org/index.php?id=emrp_calls_and_projects`; visited on August 18th 2011.

[9] A. Link, A. Täubner, W. Wabinski, T. Bruns, and C. Elster. Calibration of accelerometers: determination of amplitude and phase response upon shock excitation. *Meas. Sci. Technol.*, 17:1888–1894, 2006.

[10] B. Saggin, S. Debei, and M. Zaccariotto. Dynamic error correction of a thermometer for atmospheric measurements. *Measurement*, 30:223–230, 2001.

[11] M. Jafaripanah, B. M. Al-Hasimi, and N. M. White. Application of analogue adaptive filters for dynamic sensor compensation. *IEEE Trans. Intrum. Meas.*, 54:245–251, 2005.

[12] A. Link, B. Glöckner, C. Schlegel, R. Kumme, and C. Elster. System identification of force transducer for dynamic measurements. In *Proceedings of XIX IMEKO World Congress on Fundamental and Applied Metrology*, 2009.

[13] A. V. Oppenheim and R. W. Schafer. *Discrete-Time Signal Processing.* Prentice Hall, 1989.

[14] B. P. Lathi. *Linear systems and signals.* Oxford University Press, USA, 2005.

[15] S. Eichstädt, C. Elster, T. J. Esward, and J. P. Hessling. Deconvolution filters for the analysis of dynamic measurement processes: a tutorial. *Metrologia*, 47:522–533, 2010.

[16] C. Elster, S. Eichstädt, and A. Link. Uncertainty evaluation of dynamic measurements in line with GUM. In *XIX IMEKO World Congress on Fundamental and Applied Metrology*, 2009.

[17] A. Link and C. Elster. Uncertainty evaluation for IIR (infinite impulse response) filtering using a state-space approach. *Measurement Science and Technology*, 20, 2009.

[18] James O. Berger. *Statistical decision theory and Bayesian analysis.* Springer series in statistics. Springer, New York [u.a.], 2. ed. edition, 2006.

[19] K. Weise and W. Wöger. A Bayesian theory of measurement uncertainty. *Measurement Science and Technology*, 4:1–11, 1993.

[20] A. Papoulis and S. U. Pillai. *Probability, Random Variables and Stochastic Processes*. McGraw-Hill Series in Electrical and Computer Engineering, 2002.

[21] B. H. S. Hari and Y. R. Venugopalakrishna. On the use of dirac delta distribution in transformation of random variables. *National Conference on Communications*, 1:307–309, 2008.

[22] C. Elster and B. Toman. Bayesian uncertainty analysis for a regression model versus application of GUM Supplement 1 to the least-squares estimate. *Metrologia, in press*, 2011.

[23] I. Lira and D. Grientschnig. Bayesian assessment of uncertainty in metrology: a tutorial. *Metrologia*, 47, 2010.

[24] O. Bodnar, G. Wübbeler, and C. Elster. On the application of Supplement 1 to the GUM to nonlinear problems. *Metrologia*, in press.

[25] G. Wübbeler, P. M. Harris, M. G. Cox, and C. Elster. A two-stage procedure for determing the number of trials in the application of a Monte Carlo method for uncertainty evaluation. *Metrologia*, 47:317–324, 2010.

[26] A. Link, A. Täubner, W. Wabinski, T. Bruns, and C. Elster. Modelling accelerometers for transient signals using calibration measurements upon sinusoidal excitation. *Measurement*, 40:928–935, 2007.

[27] Y. Fujii. Measurement of the electrical and mechanical responses of a force transducer against impact forces. *Rev. Sci. Instrum.*, 77, 2006.

[28] M. Bieler, M. Spitzer, K. Pierz, and U. Siegner. Improved Optoelectronic Technique for the Time-Domain Characterization of Sampling Oscilloscopes. *CPEM Special Issue of Trans. I & M*, 1, 2008.

[29] P. D. Hale, A. Dienstfrey, J. C. M. Wang, D. F. Williams, A. Lewandowski, D. A. Keenan, and T. S. Clement. Traceable waveform calibration with a covariance-based uncertainty analysis. *IEEE Trans. Intrum. Meas.*, 58:3554–3568, 2009.

[30] S. Eichstädt, A. Link, M. Spitzer, M. Bieler, and C. Elster. Significance of correlation in the uncertainty evaluation of sampling oscilloscope measurements. In *Proceedings of IMEKO World Congress 2009, imeko2009.it.pt*, 2009.

[31] T. S. Clement, P. D. Hale, D. F. Williams, C. M. Wang, and A. Dienstfrey. Calibration of sampling oscilloscopes with high-speed photodiodes. *IEEE Trans. Microwave Theory and Techn.*, 54:3173–3181, 2006.

[32] S. M. Riad. The deconvolution problem: an overview. *IEEE proceedings*, 74:82–85, 1988.

[33] L. M. Surhone, M. T. Timpledon, and S. F. Marseken. *Wiener Deconvolution: Mathematics, Wiener Filter, Noise, Deconvolution, Frequency Domain, Signal-to-Noise Ratio, Norbert Wiener, Convolution, Impulse Response, LTI System Theory*. Betascript Publishing, 2010.

[34] A. N. Tikhonov and V. Y. Arsenin. *Solution of ill-posed problems*. John Wiley & Sons Inc. New York, 1977.

[35] P. D. Hale and A. Dienstfrey. Waveform metrology and a quantitative study of regularized deconvolution. In *IEEE Instr. and Meas. Technol. Conf. (I2MTC)*, 2010.

[36] N. Wiener. *Extrapolation, Interpolation and Smoothing of Stationary Time Series*. New York: Wiley, 1949.

[37] I. I. Gikhman and A. V. Skorokhod. On the densities of probability measures in function space. *Russ. Math. Surv.*, 21:83–156, 1966.

[38] A. V. Skorokhod. Nonlinear transformation of stochastic processes. *Kibernetika*, 2:34–40, 1966.

[39] J. van Neerven. γ-radonifying operators – a survey. *arXiv.org*, page arXiv:0911.3788v2, 2010.

[40] C. Elster and A. Link. Uncertainty evaluation for dynamic measurements modelled by a linear time-invariant system. *Metrologia*, 45:464–473, 2008.

[41] S. Eichstädt and C. Elster. *Uncertainty evaluation for continuous-time measurements*, chapter 17, page 126pp. World Scientific Publishing, 2012.

[42] D. Freedman. On the Bernstein-von Mises Theorem with infinite-dimensional parameters. *The Annals of Statistics*, 27:1119–1140, 1999.

[43] D. D. Cox. An analysis of Bayesian inference for nonparametric regression. *The Annals of Statistics*, 21:903–923, 1993.

[44] R. Christensen. Inconsistent Bayesian estimation. *Bayesian Analysis*, 4:759–762, 2009.

[45] M. Coram and S. P. Lalley. Consistency of bayes estimators of a binary regression function. *Ann. Statist.*, 34:1233–1269, 2006.

[46] S. G. Walker. New approaches to Bayesian consistency. *Statist. Sci.*, 19:111–117, 2004.

[47] C. M. Crainiceanu, D. Ruppert, and M. P. Wand. Bayesian analysis for penalized spline regression using WinBUGS. *Journal of Statistical Software*, 14, 2005.

[48] G. S. Kimeldorf and G. Wahba. Correspondence between Bayesian estimation on stochastic processes and smoothing by splines. *Ann. Math. Statist.*, 41:495–502, 1970.

[49] J. M. Bioucas-Dias. Bayesian wavelet-based image deconvolution: A GEM algorithm exploiting a class of heavy-tailed priors. *IEEE Trans. Image Processing*, 15:937–951, 2006.

[50] Brani Vidakovic. *Wavelet-based nonparametric Bayes methods*, chapter 7. Springer, 1998.

[51] T. S. Ferguson. A Bayesian analysis of some nonparametric problems. *The Annals of Statistics*, 1:209–230, 1973.

[52] A. E. Gelfand and A. Kottas. A computational approach for full nonparametric Bayesian inference under Dirichlet process mixture models. *Journal of Computational and Graphical Statistics*, 11:289–305, 2002.

[53] E. Parzen. Statistical inference on time series by RKHS methods. In *Proceedings of Canadian Mathematical Congress*, 1970.

[54] C E Rasmussen and C K I Williams. *Gaussian Processes for Machine Learning*. The MIT Press, Cambridge, Massachusetts, 2006.

[55] P. Müller and F. A. Quintana. Nonparametric Bayesian data analysis. *Statistical Science*, 19:95–110, 2004.

[56] J. L. Doob. *Stochastic Processes*. John Wiley & Sons Inc. New York, 1956.

[57] C. Shalizi. Continuity of stochastic processes. *Lecture Notes on Stochastic Processes*, CMU Department of Statistics:34–39, 2007.

[58] D. Bell. Transformation of measure on infinite-dimensional vector spaces. *Seminar on Stochastic Processes, Vancouver*, 1990.

[59] L. H. Sibul. *Application of linear stochastic operator theory*. Navy department - Naval ordnance systems command, 1968.

[60] Uwe Hassler. *Stochastische Integration und Zeitreihenmodellierung*. Springer, Berlin, 2007.

[61] R. E. Kalman and R. S. Bucy. New results in linear filtering and prediction theory. *ASME Journal of Basic Engineering*, 83:95–108, 1961.

[62] A. H. Jazwinski. *Stochastic Processes and Filtering Theory*. Dover Pubn Inc, 2007.

[63] L. P. Kadanoff. *Statistical Physics: statics, dynamics and renormalization*. World Scientific Publishing, 2000.

[64] B. Øksendal. *Stochastic Differential Equations: An Introduction with Applications*. Springer, Berlin, 2003.

[65] R. H. Cameron and W. J. Martin. Transformation of wiener integrals under nonlinear transformations. *Tr. Am. Math. Soc.*, 69, 1949.

[66] P. E. Kloeden and E. Platen. *Numerical solution of stochastic differential equations*. Springer, Berlin, 1999.

[67] T. Mikosch. *Elementary stochastic calculus with finance in view*. World Scientific Publishing, 1998.

[68] A. Girard. *Approximate Methods for the propagation of uncertainty with Gaussian Process models*. PhD thesis, University of Glasgow, 2004.

[69] C. Archambeau, M. Opper, Y. Shen, D. Cornford, and J. Shawe-Taylor. Variational inference for diffusion processes. *Neural Information Processing Systems*, 20:17–24, 2008.

[70] E. T. Whittaker. On the functions which are represented by the expansion of the interpolation theory. *Proc. Royal Soc.*, 20:199–221, 1915.

[71] C. E. Shannon. A mathematical theory of communication. *Bell Sys. Tech. J.*, 27:379–423, 1948.

[72] A. J. Jerri. The Shannon sampling theorem – its various extensions and applications: A tutorial review. *Proceedings of the IEEE*, 65:1565–1596, 1977.

[73] W. L. Briggs and V. E. Henson. *The DFT: An Owner's Manual for the Discrete Fourier Transform*. Society for Industrial and Applied Mathematics, 1995.

[74] B. Meffert and O. Hochmuth. *Werkzeuge der Signalverarbeitung*. Pearson Studium, 2004.

[75] S. Eichstädt, A. Link, P. Harris, and C. Elster. Efficient implementation of a monte carlo method for uncertainty evaluation in dynamic measurements. *submitted to Metrologia*, 2012.

[76] J. V. Candy. *Bayesian Signal Processing*. John Wiley & Sons Inc. New York, 2009.

[77] C. Stein. A two-sample test for a linear hypothesis whose power is independent of the variance. *Ann. Math. Statist.*, 16:243–258, 1945.

[78] A. Björck. *Numerical methods for least-squares problems*. SIAM, 1996.

[79] Grafakos. *Classical and Modern Fourier Analysis*. Pearson Education Inc., 2004.

[80] S. Eichstädt, A. Link, T. Bruns, and C. Elster. On-line dynamic error compensation of accelerometers by uncertainty-optimal filtering. *Measurement*, 43:708–713, 2010.

[81] S. Eichstädt, A. Link, and C. Elster. Dynamic uncertainty for compensated second-order systems. *Sensors*, 10:7621–7631, 2010.

[82] V. E. Bean, W. J. Bowers, W. S. Hurst, and G. J. Rosasco. Development of a primary standard for the measurement of dynamic pressure and temperature. *Metrologia*, 20:747, 1994.

[83] A. C. Diniz, A. B. Oliveira, J. N. Vianna, and F. J. Neves. Dynamic calibration methods for pressure sensors and development of standard devices for dynamic pressure. *Proceedings of XVIII IMEKO World Congress*, 2006.

[84] T. Esward, C. Matthews, S. Downes, A. Knott, S. Eichstdt, and C. Elster. *Uncertainty evaluation for traceable dynamic measurement of mechanical quantities: a case study in dynamic pressure calibration*, chapter 19, pages 143–151. World Scientific Publishing, 2012.

[85] H. Füser, S. Eichstädt, K. Baaske, C. Elster, K. Kuhlmann, R. Judaschke, K. Pierz, and M. Bieler. Optoelectronic time-domain characterisation of a 100 ghz sampling oscilloscope. *Meas. Sci. Technol.*, 23, Nr. 2:10pp, 2011.

[86] S. C. D. Roy. Average time delay of an analogue Butterworth filter. *Intern. Journal of Circuit Theory and Appl.*, 14:79–82, 1986.

Parts of this work have already been published in:

[15] Eichstädt, S.; Elster, C.; Esward, T. J. and Hessling, J. P. Deconvolution filters for the analysis of dynamic measurement processes: a tutorial Metrologia, 2010, 47, 522-533

[16] Elster, C.; Eichstädt, S. and Link, A. Uncertainty evaluation of dynamic measurements in line with GUM XIX IMEKO World Congress on Fundamental and Applied Metrology, 2009

[30] Eichstädt, S.; Link, A.; Spitzer, M.; Bieler, M. and Elster, C. Significance of Correlation in the uncertainty evaluation of sampling oscilloscope measurements Proceedings of IMEKO World Congress 2009, imeko2009.it.pt

[41] Eichstädt, S. and Elster, C. *AMCTM Advanced Mathematical and Computational Tools in Metrology and Testing IX* Uncertainty evaluation for continuous-time measurements, World Scientific Publishing, 2012, Chapter 17, 126pp

[80] Eichstädt, S.; Link, A.; Bruns, T. and Elster, C. On-line dynamic error compensation of accelerometers by uncertainty-optimal filtering Measurement, 2010, 43, 708-713

[81] Eichstädt, S.; Link, A. and Elster, C. Dynamic Uncertainty for Compensated Second-Order Systems Sensors, 2010, 10, 7621-7631

[85] Füser, H.; Eichstädt, S.; Baaske, K.; Elster, C.; Kuhlmann, K.; Judaschke, R.; Pierz, K. and Bieler, M. Optoelectronic time-domain characterisation of a 100 GHz sampling oscilloscope Meas. Sci. Technol., 2011, 23, 10pp

Parts of this work are already submitted for publication:

[75] Eichstädt, S.; Link, A.; Harris, P. and Elster. C. Efficient implementation of a Monte Carlo method for uncertainty evaluation in dynamic measurements, submitted to Metrologia, 2012